

I give permission for public access to my thesis and for copying to be done at the discretion of the archives' librarian and/or the College Library.


Signature

5/4/2012
Date

EXAMINATION OF THE VINYLOGOUS MANNICH REACTION
WITH A 1,3-DIKETOALDEHYDE

By

Kelsey Schramma

A thesis submitted to the faculty of Mount Holyoke College in partial fulfillment
of the requirements for the degree of Bachelor of Arts with honors

Program in Chemistry

Mount Holyoke College

South Hadley, MA

May 2012

This paper was prepared
under the direction of Dr.
Megan Nuñez for 8 credits.

Acknowledgements

My hearty thanks to Professor Christoph Schneider for giving me the opportunity to work on this project in his lab in Leipzig, Germany.

A very heartfelt thank-you to Dr. Marcel Sickert for his gracious patience and guidance in this project. His confidence in me and his kindness helped me overcome my fears of working in an organic chemistry lab and my deficiencies in the German language.

I would also like to show my immense gratitude to Professor Megan Nuñez. Her support as my academic and thesis advisor and her encouragement of all my work, both in and outside of the lab, has helped develop my confidence and scientific abilities past what I could have hoped. I am also grateful for her willingness to take me on after our first memorable meeting.

Thank you to Professor Sheila Browne, Professor Alexi Arango and Professor Darren Hamilton for being on my thesis committee.

A loving thank-you to my parents, who support everything I do and who have to put up with me calling constantly.

Thank you to my lab mates, close friends and Dina Bevivino for their support, assistance and acceptance.

Table of Contents

List of Figures	vi
Abstract	ix
1. Introduction	1
<i>1.1 Carbon-Carbon Bond Formation in Organic Synthesis</i>	<i>1</i>
<i>1.2 The Mannich Reaction</i>	<i>2</i>
<i>1.3 Vinylogous Mannich Reactions</i>	<i>5</i>
<i>1.4 The Four Main Molecules</i>	<i>9</i>
1.4.1 The Aldehyde	9
1.4.2 Amines and Imines	13
1.4.3 The Dienolate Nucleophile	16
1.4.4 The BINOL-Based Brønsted Acid Catalyst	17
<i>1.5 The Complete Vinylogous Mannich Reaction</i>	<i>20</i>
2. Methods	22
<i>2.1 Synthesis of the Aldehyde</i>	<i>22</i>
<i>2.2 Para-anisidine</i>	<i>24</i>
<i>2.3 Synthesis of the Dienolate Nucleophile</i>	<i>24</i>
<i>2.4 Synthesis of the BINOL-Based Catalyst</i>	<i>27</i>
<i>2.5 The Final Three-Component Vinylogous Mannich Reaction</i>	<i>32</i>
<i>2.6 Instrumentation and Materials</i>	<i>33</i>
3. Results and Discussion	35
<i>3.1 Identification of the Aldehyde 4-benzoyl-5-oxohexanal (22)</i>	<i>35</i>

<i>3.2 Reaction Yields of the Dienolate Synthesis and the Catalyst Synthesis</i>	46
<i>3.3 Monitoring of the Imine Formation via HPLC Analysis in the Final Vinylogous Mannich Reaction</i>	48
<i>3.4 Identification of the Cyclized Product</i>	51
4. Conclusions	68
5. References	70
6. Supplemental Material	74

List of Figures

Figure 1. The mechanism for an acid catalyzed Mannich reaction	3
Figure 2. The resonance contributors of an enol	4
Figure 3. An example of an intramolecular Mannich reaction	5
Figure 4. The vinylogous Mannich reaction with iminium ion	6
Figure 5. Proposed 3-Component Vinylogous Mannich Reaction	7
Figure 6. Detailed 3-Component Vinylogous Mannich Reaction	8
Figure 7. The Michael Reaction with Mechanism	10
Figure 8. Examples of Michael reactions	11
Figure 9. The cerium(III) chloride catalyzed Michael reaction	13
Figure 10. Imine and dienol derivatives in the vinylogous Mannich reaction	14
Figure 11. Imine protecting groups optimized by Sickert <i>et al.</i>	15
Figure 12. Alkoxy dienolates optimized by Sickert <i>et al.</i>	16
Figure 13. BINOL phosphoric acid catalysts developed by Akiyama <i>et al.</i>	18
Figure 14. The three dimensional crystal structure of the catalyst	19
Figure 15. Chiral phosphoric catalysts optimized by Sickert <i>et al.</i>	20
Figure 16. The Final 3-component vinylogous Mannich reaction	21
Figure 17. The Michael reaction from Bartoli <i>et al.</i>	22
Figure 18. The Bartoli method Michael reaction of benzoyl acetone	23
Figure 19. The reaction between oxalyl chloride and crotonic acid	25
Figure 20. The reaction of crotonyl chloride	26
Figure 21. The final step to synthesize the dienolate product	27
Figure 22. Addition of bromine to 1- <i>tert</i> -butyl-3,5-dimethylbenzene	28

Figure 23. Addition of dihydroxy borate to compound 37	29
Figure 24. Combination of boronic acid derivative to the BINOL base	30
Figure 25. Substitution of methoxy groups for hydroxy groups	31
Figure 26. Addition of the phosphoric acid to the BINOL base	32
Figure 27. The final 3-component vinylogous Mannich reaction	33
Figure 28. Aldehyde syntheses using various diketones and catalysts	36
Figure 29. The IR spectrum for the aldehyde	38
Figure 30. The ^1H -NMR spectrum for the aldehyde	40
Figure 31. Peaks from the ^1H -NMR for the aldehyde	42
Figure 32. The ^{13}C -NMR spectrum for the aldehyde	43
Figure 33. The mass spectrum for the aldehyde	45
Figure 34. The synthesis of the dienolate nucleophile with yields	46
Figure 35. The BINOL catalyst synthesis with yields	47
Figure 36. Step 1 chromatogram comparison at 220 nm	49
Figure 37. Step 2 chromatogram comparison at 220 nm	50
Figure 38. The diphenylphosphate catalyst	52
Figure 39. The ^1H -NMR spectrum for the cyclized product	53
Figure 40. The two most likely cyclizations from the chain product	56
Figure 41. The ^{13}C -NMR spectrum for the cyclized product	57
Figure 42. The ^{13}C -NMR prediction spectrum for the cyclized product	59
Figure 43. The ^{13}C -NMR prediction spectrum for the cyclized product isomer	63
Figure 44. The NOESY spectrum for the cyclized product	64
Figure 45. The mass spectrum for the final product	67

List Of Abbreviations

Ar – aromatic substituent

BINOL – 1, 1'-bi-2-naphthol

DME – dimethylether

DMF – dimethylformamide

DMPU -1,3-dimethyl-1,3-diazinan-2-one

EE – diethyl ether

ee – enantiomeric excess

GC-MS – Gas Chromatography – Mass Spectrometry

HPLC – High Pressure Liquid Chromatograph/Chromatography

IR – Infrared Spectroscopy

LDA – lithium diisopropylamide

NMR – Nuclear Magnetic Resonance

NOESY – Nuclear Overhauser Effect Spectroscopy

Nu - nucleophile

PMP – p-methoxyphenyl

TBS/TBDMS – *tert*-butyldimethylsilyl

THF – tetrahydrofuran

TLC – Thin Layer Chromatography

TMS – trimethylsilyl

UV – ultraviolet

Abstract

One of the hardest tasks in organic chemistry is the formation of a carbon-carbon bond. The synthesis of carbon-carbon bonds is crucial to the development of organic molecules such as medicines, biodegradable plastics and natural products. As such, a great deal of research has been put into developing reactions to produce these bonds. Examples of carbon-carbon bond formation reactions are the Wittig reaction, which forms a carbon-carbon double bond, the hydrophobic Grignard reaction, and the Mannich reaction. This last reaction utilizes an enolate reagent reacted with an imine to form a β -amino carbonyl. The vinylogous Mannich reaction extends the conjugation of the enolate reagent to a dienolate. This extension causes the nucleophilic carbon of the dienolate to be the γ carbon, rather than the β carbon, as seen in the Mannich reaction. The product of the vinylogous Mannich reaction is a long chained δ -amino, α,β unsaturated ketone.

The 3-component reaction, contrary to its name, has four molecules crucial to its success as a carbon-carbon bond forming reaction. The four molecules, the amine, the aldehyde, the dienolate and the catalyst, react to form the δ -amino, α,β unsaturated ketone. In our project, we synthesized a 1,3-diketoaldehyde as the aldehyde component of our 3-component reaction. It was hypothesized that the use of this aldehyde would produce a chain product that would subsequently cyclize into a hydroxyridine derivative. The first part of the two-step vinylogous Mannich reaction was the reaction of the amine, *para*-anisidine, with the

aldehyde. This reaction produced an imine intermediate. The catalyst, a BINOL-based phosphoric acid optimized by the Schneider Lab group, was added to the imine solution, as was the nucleophilic dienolate. The product of the reaction, after purification, was the anticipated cyclic hydroxyindole derivative with 83% enantiomeric excess. Further experimentation on the 3-component vinylogous Mannich reaction by varying the aldehyde can yield more complex molecules and a larger selection of possible intermediates in total syntheses.

1. Introduction

1.1 Carbon-Carbon Bond Formation in Organic Synthesis

One of the hardest reactions in organic synthesis is the formation of the carbon-carbon bond. Organic compounds, usually comprised mainly of carbon and hydrogen atoms, are found in every day life in cleaning products, natural products, and medicines. Many natural products have been discovered to have medicinal anti-bacterial, anti-tumor, and anti-cancer properties. Aspirin, for example, was originally found in tree bark and used medicinally by the Greeks and Romans before being synthetically produced in 1899.¹ The ability to synthetically produce these natural chemicals allows large quantities to be available without dependence on the plant sources. Carbon-carbon bond formation is a crucial endeavor in organic chemistry, for without the ability to synthesize carbon-carbon bonds a majority of medicines and other products would not be readily available.

Inducing two carbon atoms to form a bond with each other is particularly difficult due to their stable and nonpolar nature. Such reactions require very strong reagents and the carbons are usually unsaturated or bonded to more electronegative species, such as halogens or oxygen. In addition to forming carbon-carbon bonds, enantioselectivity between the two chiral versions of a molecule is vitally important. The two stereoisomers of a chiral molecule can

have very different chemical properties. In a chiral medicine for example, one enantiomer of the molecule in the body can have desired therapeutic effects, while the other enantiomer can have toxic effects.²

Several examples of effective carbon-carbon bond forming reactions have been developed over the past few decades. An example of a high yield (up to 99%), highly enantioselective (up to 100%) carbon-carbon bond forming reaction is the Diels-Alder reaction, which reacts a diene with a dienophile to make an unsaturated cyclohexane ring.³ Similarly, coupling reactions such as the Heck reaction and Suzuki reaction add alkenes to halide-substituted benzenes. The Friedel-Crafts reactions similarly allow carbonyl groups and alkyl chains to be attached to benzene rings. The effective Grignard reactions produce a carbanion that acts as a very strong nucleophile that, when reacted with carbonyls, forms alcohols. Michael reactions exploit the acidic nature of α -substituted carbonyls to react with an α,β -unsaturated carbonyl compound. The Mannich reaction is also useful for adding aldehydes, ketones and amines together in one reaction.

Though it appears as though there is a wealth of carbon-carbon bond forming reactions, each of these reactions has limitations. One goal of organic chemistry is to develop new reactions that can overcome these constraints.

1.2 The Mannich Reaction

Carl Mannich first recognized and developed the Mannich reaction in the early 20th century. The Mannich reaction is traditionally used to synthesize β -

amino ketones and aldehydes for pharmaceuticals and natural products. The reaction requires three different chemicals: a ketone, an amine, and an aldehyde, making it a 3-component reaction (Figure 1).

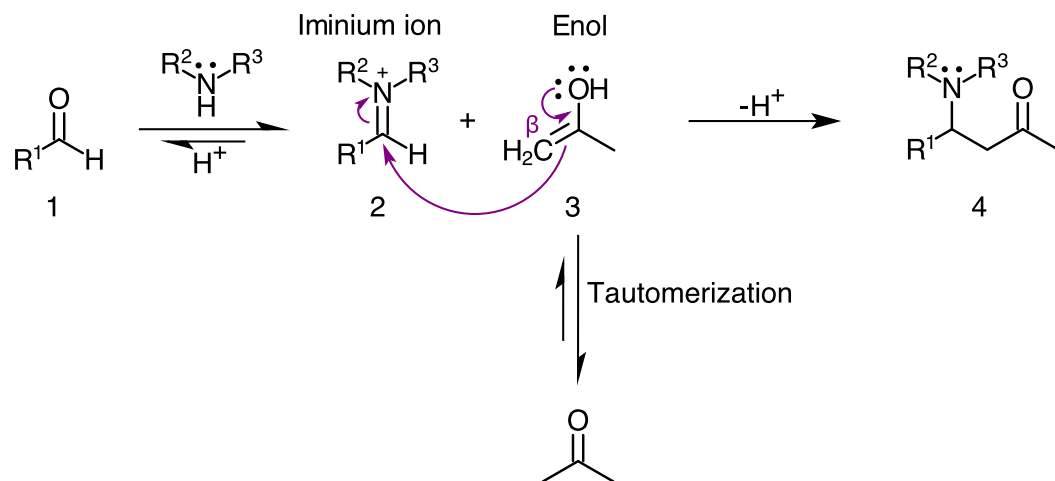


Figure 1. Mechanism for an acid catalyzed Mannich reaction from an aldehyde (1), an amine and a ketone, which reacts in the enol arrangement (3).

The 3-component reaction takes place in two steps, starting with a reaction between the aldehyde (1) and the amine. The nitrogen of the amine attacks the carbonyl of the aldehyde and undergoes an imine formation. This replacement of the oxygen with the nitrogen forms the iminium ion (2) and water. The equilibrium of this reversible reaction is generally favored towards the imine form of the molecule. This preference is a result of more basic nature of nitrogen over oxygen. Because nitrogen is more basic than oxygen, it is more likely to interact with the carbonyl than the oxygen with the formed imine.⁴

The second step of the reaction occurs upon addition of the ketone. Ketones are naturally in equilibrium with a more reactive enol form through the process tautomerization (Figure 1). The resonance contributors of the enol form demonstrate why the form is less stable than the keto form (Figure 2). One resonance contributor of the enol form has a double bond with an alcohol as a substituent. The other resonance contributor to this form however, can be represented by a protonated carbonyl and an unstable carbanion. The resonance hybrid of these two contributors has some carbanionic character at the β position, which allows this carbon to be a nucleophile and more reactive. When the ketone is in its enol form (3), this carbanion acts as strong nucleophile and it is this reactive species that attacks the positively charged iminium carbon in the Mannich reaction.

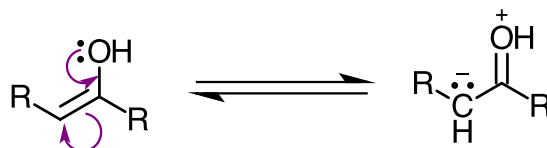


Figure 2. The resonance contributors of an enol.

The Mannich reaction is extremely useful in organic synthesis, but has several disadvantages. The reaction times are long (up to several days) and many side products are formed. Ketones with two reactive α -positions lead to bis-Mannich bases and regioselectivity of the reaction is difficult to control.⁵ Intramolecular Mannich reactions, however, are very useful in natural product synthesis and are gateways to creating complex regio- and stereoselective molecules. Figure 3 shows an example of an intramolecular Mannich reaction for

synthesizing polysubstituted piperidines, where the amine and the enolizable ketone are functional on the same molecule, which subsequently reacts with the aldehyde.⁶

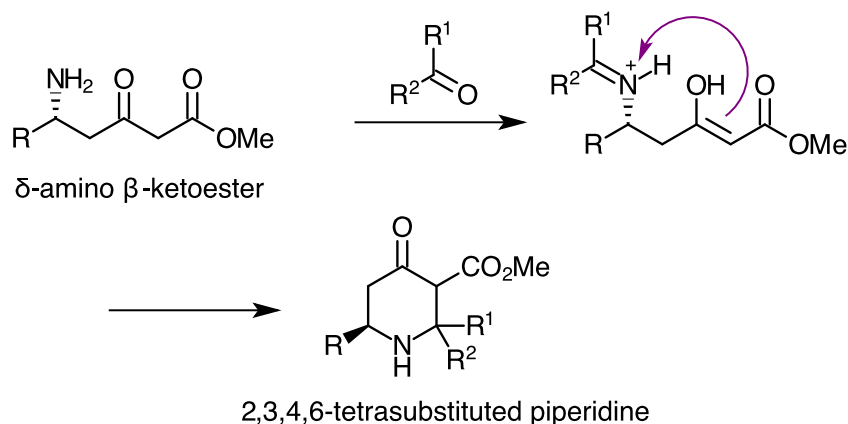


Figure 3. An example of an intramolecular Mannich reaction, synthesizing polysubstituted piperidines.⁶

1.3 Vinylogous Mannich Reactions

The vinylogous Mannich reaction is a valuable carbon-carbon-bond-forming process that is often used in organic synthesis to make new molecules, such as natural products and organic intermediates. This reaction extends the Mannich reaction by adding a reactive vinyl group to the ketone group (6) and also gives chemists the ability to synthesize complex and highly functionalized compounds that would normally be difficult or sometimes impossible to synthesize. This C-C bond forming reaction is produced through the addition of

an aldehyde, an amine and a dienolate nucleophile, which react with a catalyst to form an δ -amino α,β -unsaturated carbonyl compound (7 in Figure 4).

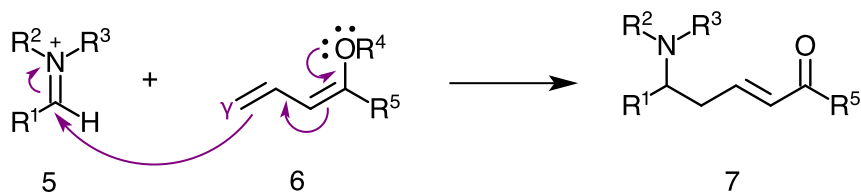


Figure 4. Vinylogous Mannich reaction with iminium ion (5) and dienolate (6) produce a δ -amino α,β -unsaturated carbonyl product (7).

The process for forming the iminium ion (5) or imine is the same as the canonical Mannich reaction; however, the enol of the Mannich reaction is replaced by an enolate, which is then extended to a dienolate by adding a conjugated double bond, or vinyl group (6). The group attached to the enolate R^4 is deliberately a large stable leaving group, since it needs to be removed to induce the electrons on the oxygen to move down to form a carbonyl. In this reaction, the electrons that form the bond between the two compounds come from the double bond between the β and γ carbons on the dienolate. The dienolate γ carbon attaches to the iminium carbon, creating the δ -amino α,β -unsaturated carbonyl product. Figure 5 shows the four primary molecules used in the 3-component vinylogous Mannich reaction: the aldehyde (8), the amine (9) (*para*-anisidine), the dienolate nucleophile (10), and the catalyst (11). The last, though not one of the “three components,” activates the imine to make a more electrophilic and reactive imine carbon; this catalyst is therefore necessary for the reaction to proceed.

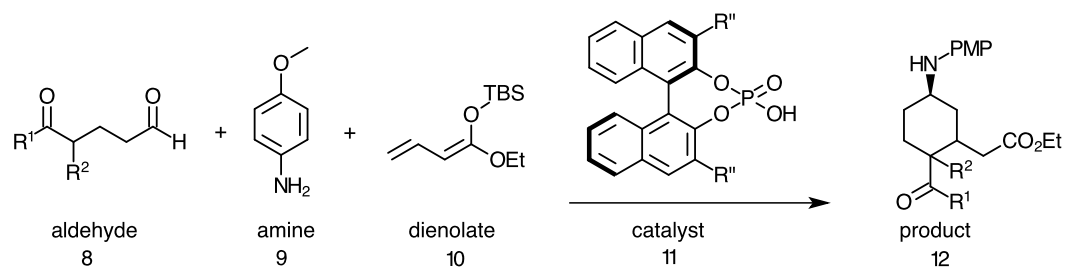


Figure 5. Proposed 3-Component Vinylogous Mannich Reaction

As seen in the Mannich reaction and the vinylogous Mannich reaction, the aldehyde reacts with the amine to form an imine. The imine then reacts with the dienolate through catalytic activation. The product of this reaction then cyclizes to form the final product (12). Figure 6 shows a more detailed version of Figure 5, including the chain intermediate as well as substituent groups on the aldehyde as described by Sickert *et al.*⁷ The p-methoxyphenyl group (PMP), a protecting group, ensures that the amine does not react in the given reaction. This group can be added and removed later to reinstate the reactivity of the nitrogen.

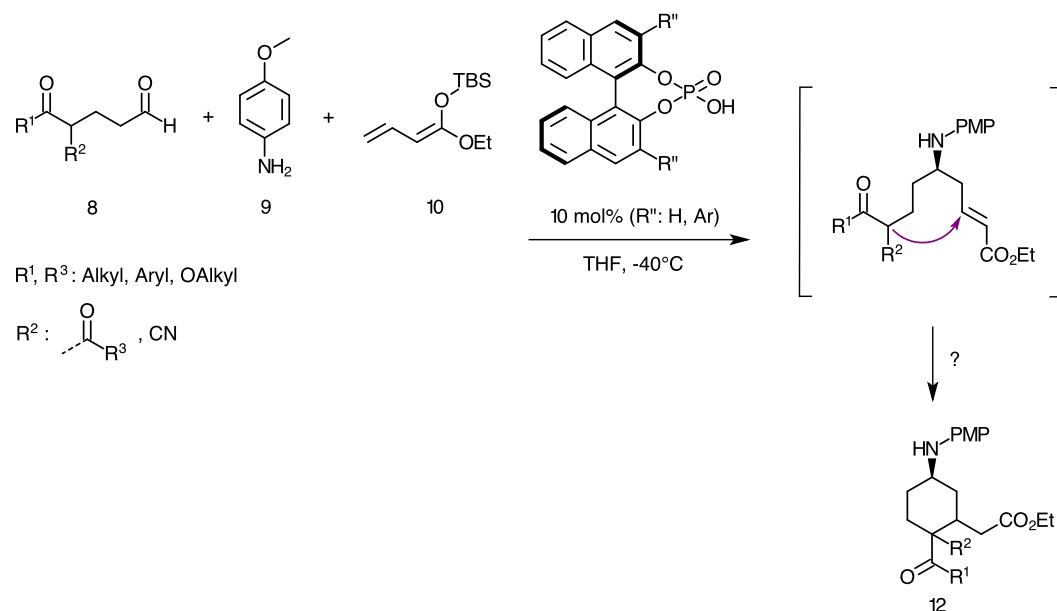


Figure 6. Detailed 3-Component Vinylogous Mannich Reaction

Sickert *et al.* varied each of the reactants in the 3-component vinylogous Mannich reaction investigating what kinds of products, yields and enantioselectivities would result from the variations. For example, Sickert *et al.* varied the substituent groups (R^1 and R^2) on the aldehyde between alkyls, aryls (aromatic substituents), and alkoxy groups (-OAlkyl). R^2 was also substituted by oxo (ketone) groups and nitriles.⁷

The catalyst used in this 3-component reaction is based on 1,1'-bi-2-naphthol (BINOL), with the phosphorus center acting as a Brønsted acid catalyst. Sickert *et al.* also varied the substituent group (R'') on this catalyst from a simple hydrogen to an aromatic substituent.⁷ This vinylogous Mannich reaction results in a chain product, which is an intermediate to the final cyclized product (12), though the process of cyclization has not yet been determined. The cyclization seen in Figure 6 is not representative of every cyclization possible for this

reaction. The favored cyclization for each product depends heavily on the aldehyde substituent groups (R^1 and R^2).

This thesis reports the variations we made to the substituent groups on the aldehyde. Once a stable high-yielding aldehyde was found, we used that aldehyde in the 3-component reaction to form a cyclized product. This reaction and its derivatives form products with good stereoselectivity and relatively high yields.

1.4 The Four Main Molecules

1.4.1 The Aldehyde

The research lab group of Professor Schneider works to elucidate the wide variety of possible products from the 3-component vinylogous Mannich reaction. One branch of this project involves varying the aldehyde used. In this experiment, we varied the R^2 substituent on the aldehyde (8) with oxo-groups, or ketones. Our initial goal was to find a reaction that produced a high yield of aldehyde product. To accomplish this goal, we utilized the Michael reaction to bind varying 1,3-diketones to the aldehyde acrolein.

1.4.1.1 The Michael Reaction

Named after Arthur Michael who first described this reaction, the Michael reaction creates a C-C bond between an enolate, or unsaturated carbonyl group, and a nucleophile (Figure 7). This reaction is a high-yield, efficient method of C-C-bond formation and is used widely in organic synthesis and biosynthesis.

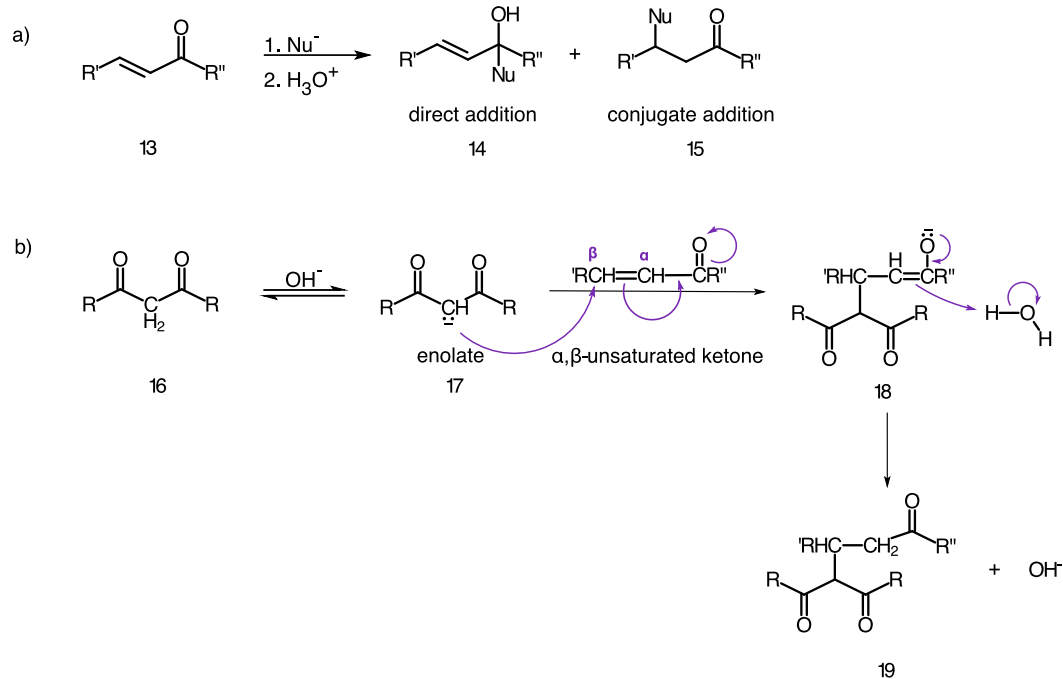


Figure 7. a) General Michael reaction using an α,β unsaturated ketone (13) resulting in direct and conjugate additions; b) Mechanism for the Michael reaction with a β -diketone (16) producing a conjugate addition product.

Figure 7a gives a general Michael reaction with an α,β -unsaturated ketone (13). A nucleophile, often an enolate ion (17), reacts with either the carbonyl group of the aldehyde, as seen in the direct addition (14), or with the conjugated double bond, which leads to the conjugate addition (15). The major products of Michael reactions are usually the conjugate addition due to the low reactivity of the carbonyl group and the weak basicity of the enolate ion.

Figure 7b shows the mechanism for the Michael reaction. The carbon between two carbonyls is a weak acid, ranging in pK_a value from 5.9 to 13.3 depending on the substituents.⁴ A base can remove one of the protons from the

diketone (16) and form the enolate ion (17). The α -carbon on the enolate ion adds to the β -carbon on the α,β -unsaturated ketone. The nucleophilic α -carbon of the carbonyl is then protonated from the solvent (18), re-creating the base catalyst from the beginning and creating a 1,5-dicarbonyl compound (19).

The enolate ion in a Michael reaction works most ideally with two electron withdrawing groups. Some examples of such groups are β -diketones, β -diesters, β -keto nitriles and β -keto esters (Figure 8). Similarly, the unsaturated carbonyl group can also be varied between unsaturated ketones, amides, esters and rarely aldehydes.^{4,8}

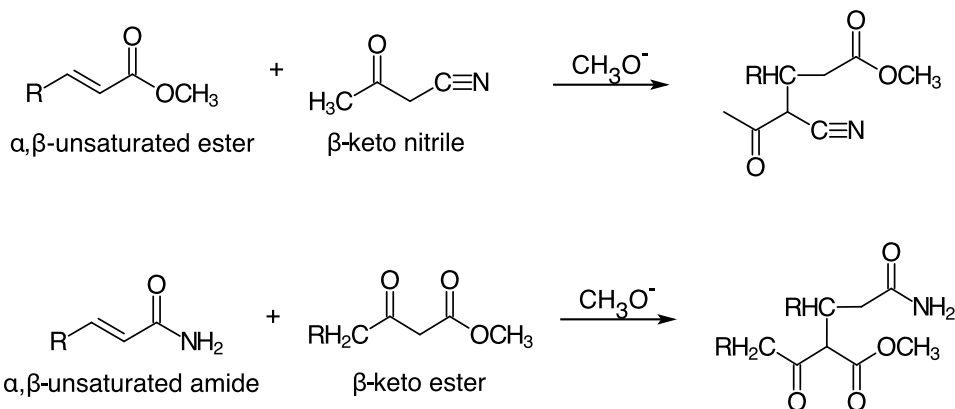


Figure 8. Examples of Michael reactions with an α,β -unsaturated ester and an α,β -unsaturated amide acting as the unsaturated carbonyl group and a β -keto nitrile and a β -keto ester acting as the respective nucleophile.⁴

The strongly basic conditions of the Michael reaction often result in side products of polymerization, self-condensation and rearrangements. One inexpensive Michael reaction synthesis under less harsh conditions exploits cerium(III) chloride and a Lewis acid catalyst. The catalyst $\text{CeCl}_3 \cdot 7\text{H}_2\text{O}/\text{NaI}$, for

example, has been developed by Bartoli *et al.* in Michael reactions between an aldehyde and indoles⁹ or amines¹⁰. The cerium(III) chloride catalyzed Michael reaction in the presence of sodium iodide produces high yields of the Michael addition between 1,3-dicarbonyl compounds and α,β -unsaturated ketones and aldehydes at room temperature under relatively mild conditions with few polymerizations and self-condensations.¹¹

In his paper detailing the cerium(III) chloride catalyst, Bartoli reported that performing the Michael reaction without the Lewis acid NaI was slow and yielded poor results. He observed that NaI increases the efficiency of the $\text{CeCl}_3 \cdot 7\text{H}_2\text{O}$ and in the proper proportions caused the reaction to go to completion after only a few hours. Performing the experiment without solvent (providing one of the reagents was in liquid form) also shortened the reaction time of the Michael addition and allowed the catalyst to be recovered without any loss of activity. The mild conditions of the $\text{CeCl}_3 \cdot 7\text{H}_2\text{O}/\text{NaI}$ and room temperature are ideal for preventing polymerization of reagents that are susceptible to polymerization, such as methyl vinyl ketone (also known as acrolein).¹¹ Unfortunately the mechanism of the $\text{CeCl}_3 \cdot 7\text{H}_2\text{O}/\text{NaI}$ catalyzed reaction is unknown.

1.4.1.2 Synthesizing the Aldehyde

In this project, we performed the Michael reaction with several different 1,3-dicarbonyls and the α,β -unsaturated ketone acrolein (21) following Bartoli's method of using cerium(III) chloride in the presence of sodium iodide. 4-benzoyl-5-oxohexanal (22 in Figure 9) from the diketone benzoyl acetone (20) was the most successful aldehyde produced due to the best yield and fewest side products.

We used this aldehyde (22) in the final 3-component vinylogous Mannich reaction.

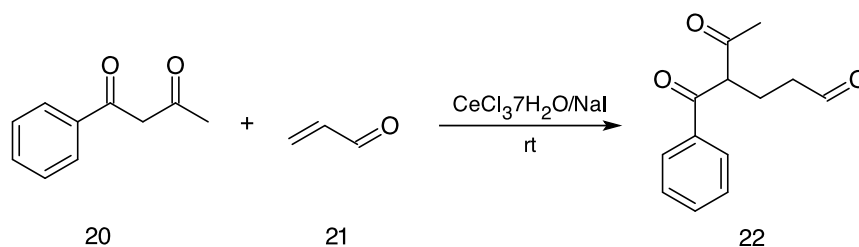


Figure 9. A cerium(III) chloride catalyzed Michael reaction in the presence of NaI between the diketone benzoyl acetone (12) and the α,β -unsaturated aldehyde acrolein (13) to produce a 1,3-diketo substituted aldehyde.

1.4.2 Amine and Imine

In the 3-component vinylogous Mannich reaction, one of the three components is an amine. However, in this reaction, the nitrogen of the amine needs to be in the form of an imine to react. In our case, we combined the aldehyde with the amine to create the imine, but this is not always the case. Many examples of vinylogous Mannich reactions start with an imine or iminium ion.^{12,13,14}

Because the vinylogous Mannich reaction has a wide range of synthetic uses, the amine or imine used in the reaction varies depending on the application. For example, Martin used several cyclic imines in vinylogous Mannich syntheses to produce cyclic alkaloids.¹² Zhang *et al.* used 2-aminophenol reacted with an aldehyde in their vinylogous Mannich reaction consistently with N,N'-dioxide-

scandium(III) catalyst complex.¹⁵ Another experiment by Liu *et al.* exploited an imine with *tert*-butyl carbamate protecting groups.¹³

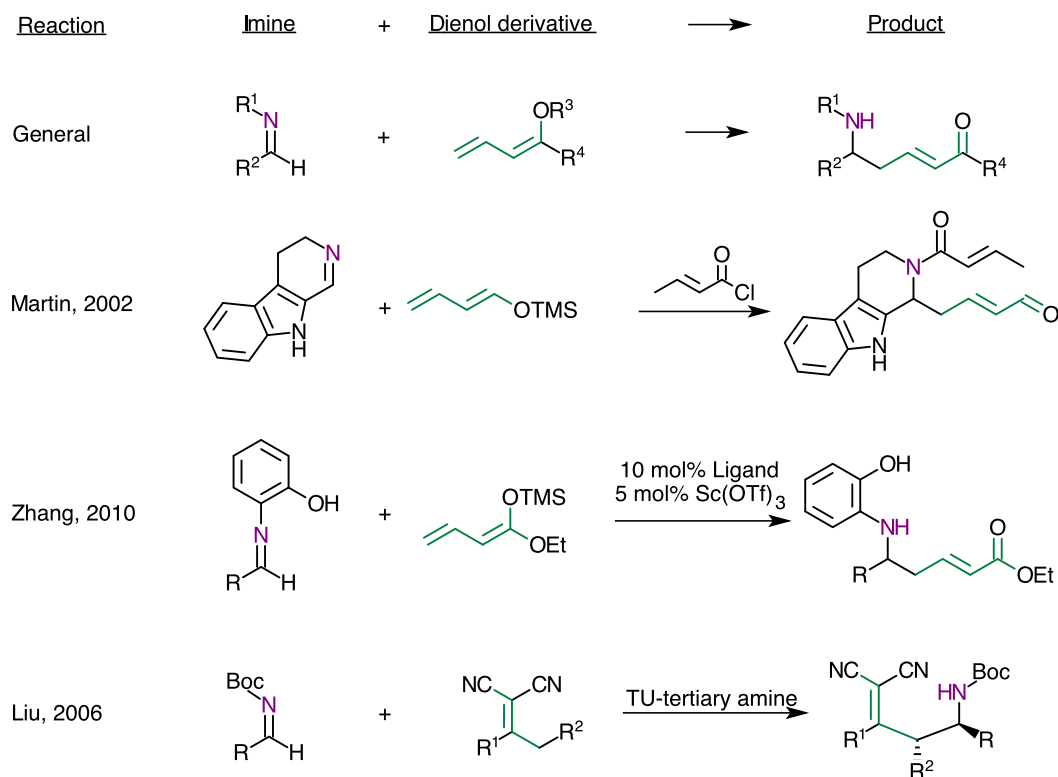


Figure 10. Examples from the primary literature of imines and dienol derivatives in the vinylogous Mannich reaction.^{12,13,15}

Sickert *et al.* also experimented with different protecting groups on the formed imine, which is the product of step one of the vinylogous Mannich reaction.⁷ The protecting group ensures that the nitrogen of the imine does not react. Though it can be removed after the reaction, its presence can affect the reactivity and stereochemistry of the reaction. Sickert's goal was to determine

which protecting group resulted in the highest yield of product from the vinylogous Mannich reaction.

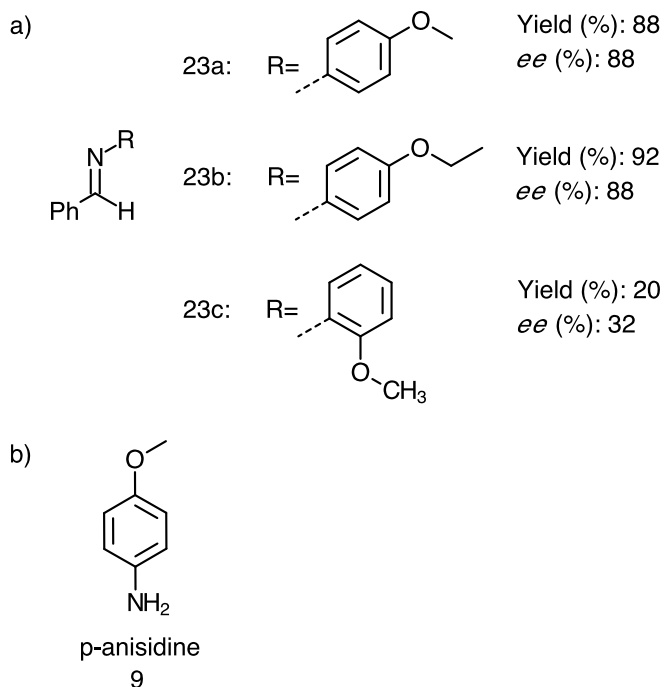


Figure 11. a) Imine protecting groups optimized by Sickert *et al.* that protect the reactivity of the imine in the 3-component vinylogous Mannich reaction. b) The final amine *para*-anisidine used in our vinylogous Mannich reaction.⁷

The most effective groups were found to be *p*-ethoxyphenyl (23b) and *p*-methoxyphenyl (23a). It was observed that *para*-substituted phenyl groups produced higher yields and better stereospecificity than *ortho*-substituted phenyl groups. The *p*-methoxyphenyl substituted amine, or *p*-anisidine (9), was less expensive than the *p*-ethoxyphenyl, and since both yielded similar results, we used *p*-anisidine in the 3-component reaction in this project.

1.4.3 The Dienolate Nucleophile

The third component of the 3-component reaction after the aldehyde and the amine is the dienolate. As detailed above, the enol form of the molecule is crucial to its reaction and several papers have shown that the dienolates usually react in to form a conjugate addition product. The oxygen on the dienolate is bonded to a large substituent that acts as a leaving group in the vinylogous Mannich reaction. Some commonly used leaving groups are silyl ethers, such as trimethylsilyl (TMS) and *tert*-butyldimethylsilyl (TBS/TBDMS).

Several examples of dienol derivatives are seen in Figure 10. Martin showed a fairly traditional dienol derivative in his review of alkaloids.¹² Zhang *et al.* experimented with acyclic silyl dienol esters, also a traditional form.¹⁵ Liu *et al.* however completely forewent the traditional form of the dienol and instead used an R,R-dicyanoolefin, which contains two nitrile groups on an olefin.¹³ Other variations on the dienolate form include adding substituents to the double bonds¹⁶ and the central enol carbon, as seen in Figure 12.⁷

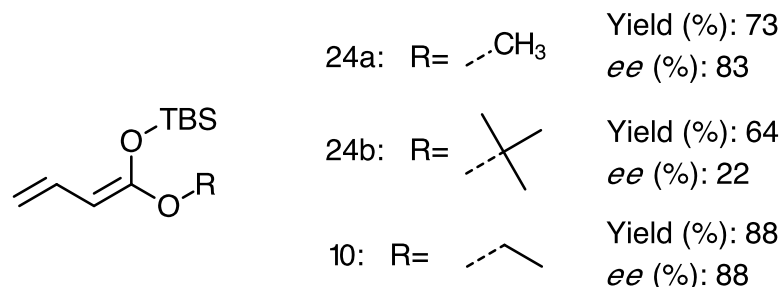


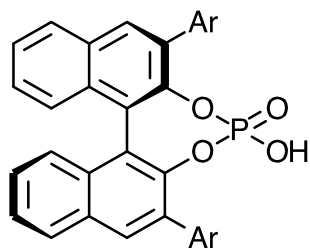
Figure 12. Alkoxy dienolates optimized by Sickert *et al.* which act as a nucleophile in the 3-component vinylogous Mannich reaction.⁷

Sickert *et al.* determined that small alkoxy groups on the dienolate produced higher enantioselectivities up to 88% *ee* (enantiomeric excess) with ethoxy (10) and 83% with methoxy (24a) (Figure 12). Their larger counterparts, such as *tert*-butoxy (24b), only produced 22% *ee* and gave 64% yield.⁷ The ethoxy-substituted dienolate with a TBS group on the enolate was used for our vinylogous Mannich reaction (10).

1.4.4 BINOL-Based Brønsted Acid Catalyst

Acids and bases catalyze many reactions, where there is usually a proton transfer between the catalyst and the reactant. Brønsted acids typically donate a proton to the reaction and do not lend stereospecificity to the reaction. In organic synthesis reactions however, it is crucial to have stereospecific products due to the differing effects of chirality. In the past decade, small organic molecules have been developed for use as catalysts. These organocatalysts offer inexpensive and less hazardous catalysts than their metal counterparts. Several have been developed for use as stereospecific catalysts.^{17,18,19,20}

Sickert *et al.* reported a catalytic, enantioselective vinylogous Mannich reaction in 2008 of acyclic dienolates with imines catalyzed by a chiral Brønsted acid.¹⁷ The catalyst they were interested in was a large BINOL-based catalyst (Figure 13) developed by Akiyama *et al.* in 2004.²⁰



25a: Ar=H

25b: Ar=C₆H₅

25c: Ar=2,4,6-Me₃C₆H₂

25d: Ar=4-MeOC₆H₄

25e: Ar=4-NO₂C₆H₄

Figure 13. BINOL-based phosphoric acid catalysts developed by Akiyama *et al.* for an enantioselective Mannich reaction.²⁰

This chiral molecule is capable of catalyzing a stereospecific reaction due to its large aromatic groups. The connected naphthalene-like groups sterically prevent the molecule from inversion at the heterocyclic ring in the center of the molecule. The molecule is essentially locked in place, so the catalytic phosphoric center is stereospecifically rigid. The three-dimensional picture of a BINOL-based phosphoric acid can be seen in Figure 14.

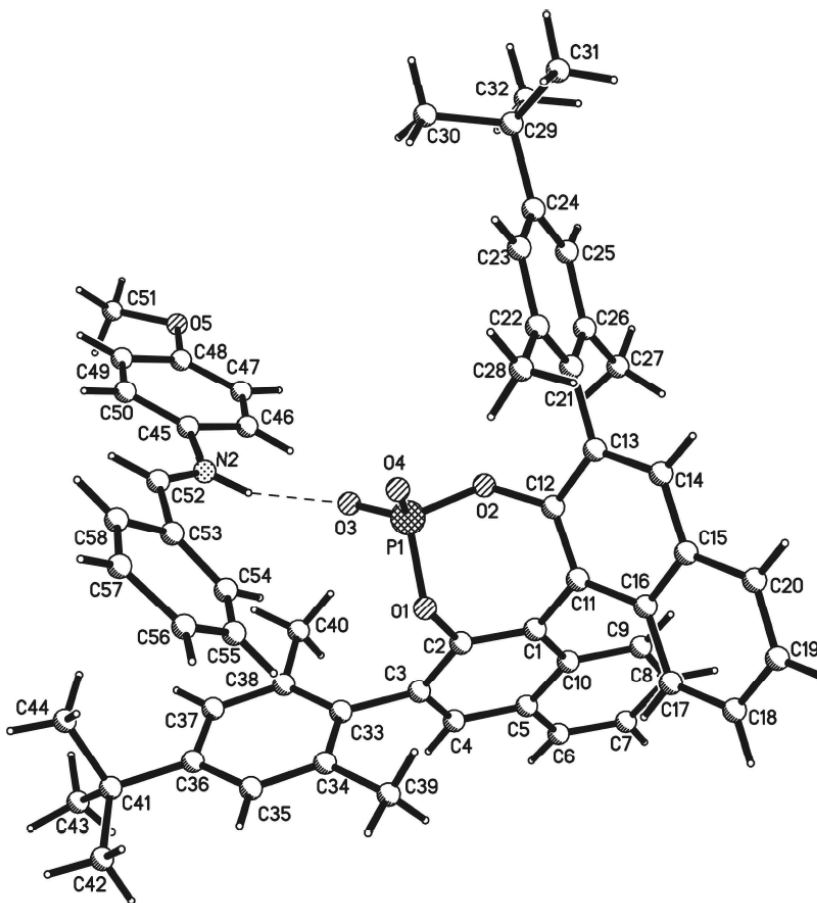


Figure 14. Three dimensional crystal structure representation of the BINOL-based phosphoric acid used in the 3-component vinylogous Mannich reaction.⁷

Akiyama *et al.* experimented with substituent groups at the 3,3' position of the molecule in a Mannich reaction²⁰, which contributed to increasing the yield and enantiomeric excess of the formed product. Sickert *et al.* used similar experiments with the vinylogous Mannich reaction with the result that these Brønsted acid catalysts produced excellent yields (88-96% for most cases) and high enantioselectivity, usually above 90% *ee* and above 95% in select cases.⁷

Figure 15 below shows the three most enantioselective and high yielding catalysts investigated by Sickert.

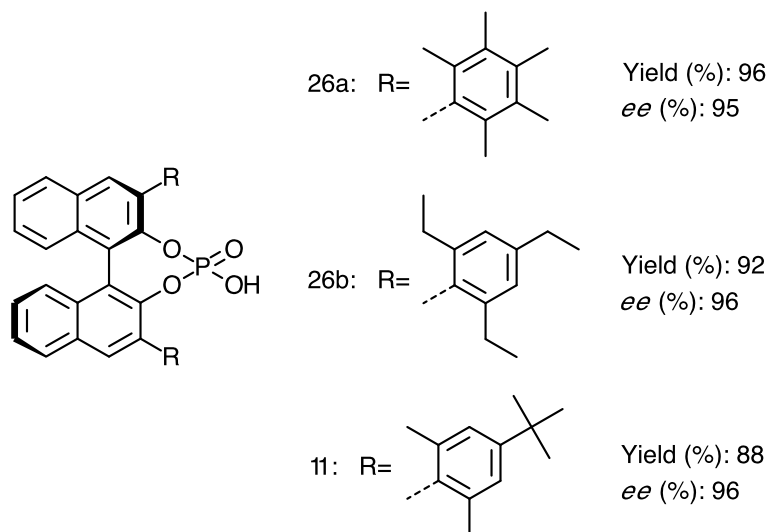


Figure 15. Chiral phosphoric Brønsted acidic catalysts optimized by Sickert *et al.*⁷

The BINOL-based catalyst used in our project had the 2,6-methyl-4-*t*-butyl phenyl group (11).

1.5 The Complete Vinylogous Mannich Reaction

The vinylogous Mannich reaction detailed in this thesis was carried out using the four optimized compounds described above: the aldehyde, the amine, the dienolate nucleophile and the BINOL catalyst. We synthesized each of these molecules and performed the 3-component vinylogous Mannich reaction. The aldehyde (22) was combined with the amine (9) to form an imine intermediate, as seen in Figure 16. The dienolate nucleophile (10) was then added to the

unpurified imine along with the BINOL catalyst (11). We hypothesized that these four components together would produce the carbon-carbon bond desired and the product of our vinylogous Mannich reaction would be a chain product (27) that would subsequently cyclize (28). After performing the reaction, we were able to confirm the presence of this predicted cyclic product with 83% *ee*.

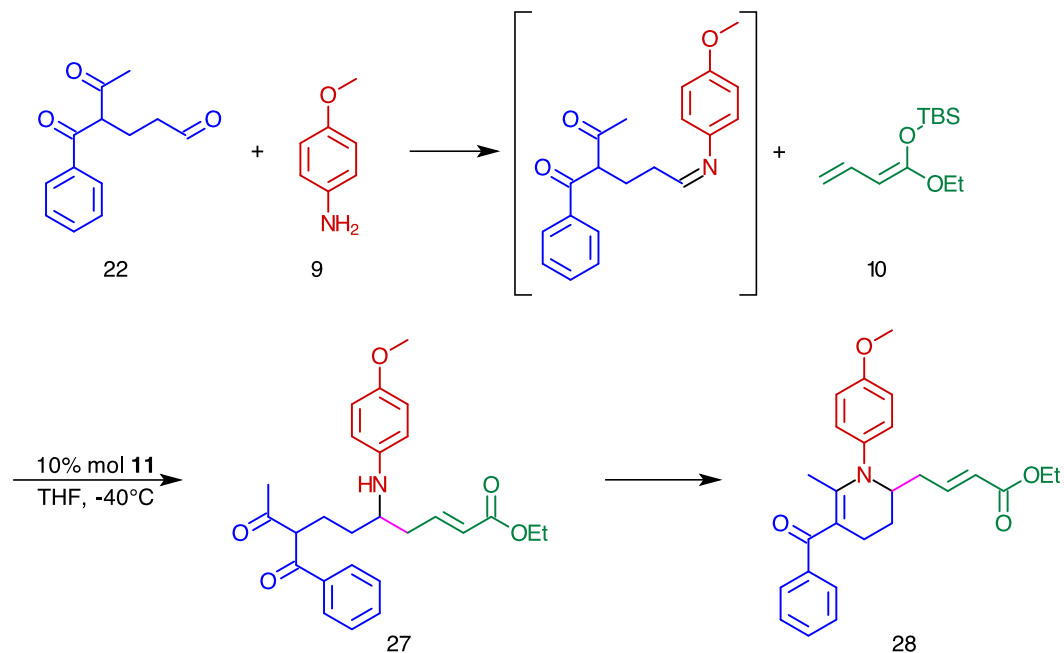


Figure 16. Thesis 3-component vinylogous Mannich reaction with aldehyde (22), amine (9), dienophile nucleophile (10) and the catalyst (11) to form the chain product (27), which then cyclized to the final product (28). The formed carbon-carbon bond is in pink.

2. Methods

Before the final vinylogous Mannich reaction could be performed, the four molecules in the reaction were chemically synthesized independently.

2.1 Synthesis of the Aldehyde

The Michael reaction protocol from Bartoli was used to synthesize a 1,3 diketoaldehyde from a 1,3 diketone and the aldehyde acrolein (Figure 17).¹¹ We experimented with several different 1,3 diketones to find which would produce the highest and purest yields.

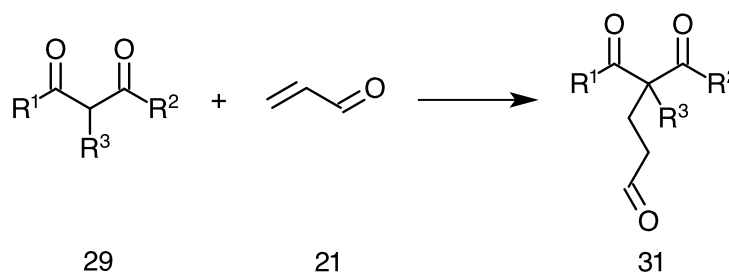


Figure 17. The Michael reaction from Bartoli *et al.*¹¹ A 1,3 diketone (29) reacts with the aldehyde acrolein (21) to form a 1,3 diketoaldehyde (31).

The Bartoli method included directly mixing the 1,3 diketone, acrolein and the catalyst $\text{CeCl}_3 \cdot 7\text{H}_2\text{O}/\text{NaI}$ in a test tube without solvent overnight or until the product congealed in the test tube.¹¹ We then compared the reactants to the products using thin layer chromatography (TLC). The 1,3 diketone which

produced the highest yield was benzoyl acetone, which yielded 4-benzoyl-5-oxohexanal (Figure 18).

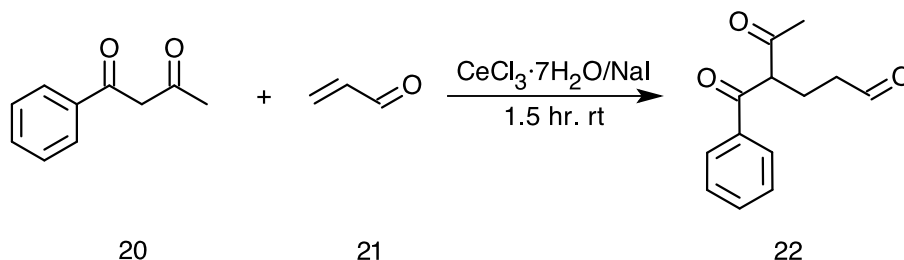


Figure 18. The Bartoli method Michael reaction of benzoyl acetone (20) with acrolein (21) in the presence of catalyst $\text{CeCl}_3 \cdot 7\text{H}_2\text{O}/\text{NaI}$ to form the diketoaldehyde product (22).¹¹

This product was formed by adding 162.188 mg (1 eq., 1 mmol) of benzoyl acetone, 61.6704 mg (1.1 eq., 1.1 mmol) of acrolein (prop-2-enal), 74.517 mg (0.2 eq., 0.2 mmol) of cerium(III) chloride heptahydrate and 14.989 mg (0.1 eq., 1.1 mmol) of sodium iodide in a test tube. This mixture was stirred at room temperature under argon. The reaction congealed after 1.5 hours and some dichloromethane (3-5 mL) was added to the test tube. The catalyst mixture was removed by vacuum filtration and rinsed with dichloromethane (CH_2Cl_2). The filtered extracts were concentrated under reduced pressure and the crude yellow colored product was monitored by thin layer chromatography and purified by silica gel chromatography (EE (diethylether):hexane – 1:3). The product was identified through $^1\text{H-NMR}$ (nuclear magnetic resonance), $^{13}\text{C-NMR}$, GC-MS (Gas chromatography-mass spectrometry) and IR (Infrared spectroscopy).

Other diketones were tried using the same Bartoli method, including diethyl methyl malonate, diethyl malonate, and ethyl acetoacetate. These reactants however formed many side products, as seen on the TLC and NMR spectra taken from the column-separated samples, and were rejected for further testing. Similarly, another Michael reaction method was tried according to Noël *et al.* which combines the 1,3 diketone with acrolein and the catalyst Al_2O_3 at 0°C .²¹ This method however produced many different products and little yield, and was therefore dismissed. The purified aldehyde (22) was refrigerated until needed in the final reaction. The aldehyde did show signs of some self-polymerization, but the evidence was not significant enough to merit re-purification.

2.2 *Para*-anisidine

The amine *p*-anisidine was supplied from Acros (99%) and did not need to be purified further.

2.3 Synthesis of the Dienolate Nucleophile

The dienolate nucleophile 1-(*tert*-butyldimethylsilyloxy)-1-ethoxy-1,3-butadiene was synthesized according to procedures already developed and optimized by the Schneider lab group. The first part of the synthesis was to synthesize crotonyl chloride (34). In a flask at 0°C under argon gas, 87.2 mL (128.93 g, 1.0 mol, 1.0 eq.) of oxalyl chloride (32) was carefully added to 86.0 g

(1.00 mol, 1.0 eq.) of crotonic acid (33) within 15 minutes and was left to stir under gas for 1-2 hours at 0°C. A few drops of dimethylformamide (DMF) were added and the resulting translucent brown mixture was let stir overnight at room temperature. An NMR was taken to ascertain the purity of the product. The mixture of crotonyl chloride (34) was further synthesized without purification.

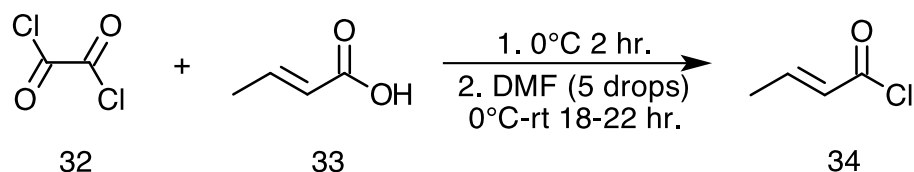


Figure 19. The reaction between oxalyl chloride (32) and crotonic acid (33) to form crotonyl chloride (34).

We added 16.0 mL (12.5 g, 0.273 mol, 1.40 eq.) of ethanol and 30.0 mL (21.8 g, 0.216 mol, 1.10 eq.) of NEt_3 to 100 mL (71.34 g, 0.195 mol, 1.0 eq.) absolute Et_2O at 0°C. 18.4 mL (20.0 g, 0.191 mol, 1.00 eq.) crotonyl chloride (34) was then added to the solution dropwise over 45 minutes and stirred for 1-2 hours at 0°C. The resulting white ammonium salt (HNEt_3Cl) was filtered out and washed with ice-cold Et_2O . The solvent was concentrated under decreased pressure (100 mbar, 40 °C) and the raw product was purified by distillation over a 5 cm Vigreux Column.

The products of this reaction were unsaturated esters, with the double bond in either the α - β position or the β - γ position (Figure 20). Both of the acetic acid ethenyl products (35) were used in the next reaction to synthesize the final dienolate product (10).

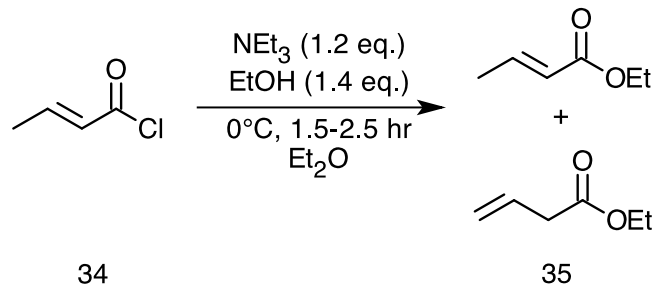


Figure 20. The reaction of crotonyl chloride (34) in a solution of ethanol (EtOH), triethylamine (NEt₃), diethyl ether (Et₂O) to form two unsaturated esters (35).

Continuing the synthesis to the final dienolate product, we added 38.0 mL (96.0 mmol, 2.5 M in hexane, 1.20 eq.) n-butyllithium to a solution of 12.3 mL (8.88 g, 87.9 mmol, 1.10 eq.) diisopropylamine (*i*-Pr₂NH) and absolute THF (0.7M) dropwise within 10 minutes at 0°C. This mixture made lithium diisopropylamide (LDA). The solution stirred for 30 minutes at 0°C. Afterwards, the reaction was cooled to -78°C and 11.6 mL (12.3 g, 96.0 mmol, 1.20 eq.) 1,3-dimethyl-1,3-diazinan-2-one (DMPU) was added within 10 minutes. We stirred the resulting cloudy mixture for 45 minutes. We then added 10.0 ml (9.20 g, 80.0 mmol, 1.0 eq.) of the unsaturated esters (35) (dissolved in 20 mL/0.1 mol abs. THF) dropwise to the mixture within 30 minutes at -78°C and stirred it for 2 hours. Afterwards, we added 15.0 g (100 mmol, 1.25 eq. dissolved in 20 mL/0.1 mol abs. THF) of TBS-Cl to the resulting yellow solution within 30-60 minutes, and stirred it for 15 minutes at -78°C and further stirred for 2 hours at room temperature. We subsequently extracted the reaction mixture with petroleum ether (400 mL/0.1 mol), washed it with ice water (4x per 400 mL/0.1 mol) and dried the

mixture with MgSO₄. The solution was then concentrated under reduced pressure and the resulting oil was kept at 55°C and 1 mbar for 3 hours. We distilled the remaining dienolate raw product (10) over a 5 cm Vigreux Column. The product was confirmed by ¹H-NMR.

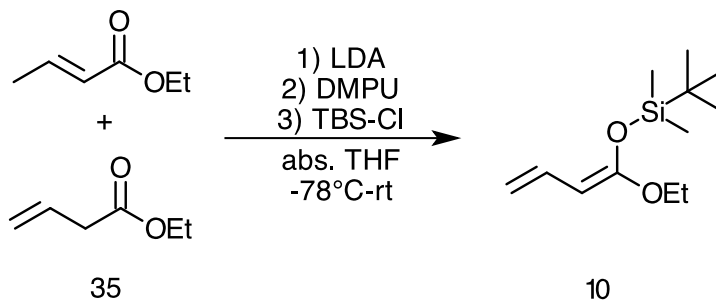


Figure 21. Final step to synthesize the dienolate product (10) from the unsaturated esters (35) and the addition of LDA, DMPU, and TBS-Cl.

The final clear liquid dienolate product (10) was kept in a -20°C freezer until needed for the vinylogous Mannich reaction.

2.4 Synthesis of the BINOL-Based Catalyst

The BINOL-based catalyst was synthesized according to protocols optimized by the Schneider lab group. To create the catalyst ((R)-3,3'-bis(4-*tert*-butyl-2,6-dimethylphenyl)-1,1'-binaphthyl-2,2'-diyl)-hydrogenphosphate (11), we began by dropping a solution of 9.10 mL (25.6 g, 0.160 mol, 1.0 eq.) of Br₂ in 19.0 mL CHCl₃ into a solution of 30.0 mL (26.0 g, 0.160 mol, 1.0 eq.) of 1-*tert*-

butyl-3,5-dimethyl benzene (36) and 0.30 g (5.4 mmol, 3 mol%) of Fe in 25 mL CHCl₃ at 0°C within 1 hour. We stirred the resulting mixture at 0°C for 2 hours. Subsequently, we transferred the mixture into diluted 1N NaOH (100 mL/0.1 mol) and treated it with solid Na₂SO₃ until the solution turned transparent. The mixture was extracted with CH₂Cl₂ (3x for 80 mL/0.1 mol). We then extracted the collective organic phases with a diluted 1N NaOH (150 mL/0.1 mol) and then washed them with a Na₂SO₃ solution (150 mL/0.1 mol) and dried the solution with MgSO₄. The product (37) was concentrated under reduced pressure and crystallized under hexane.

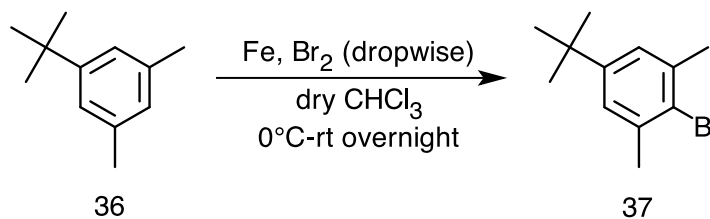


Figure 22. Addition of bromine to 1-*tert*-butyl-3,5-dimethylbenzene (36) to form 5-*tert*-butyl-2-bromo-1,3-dimethylbenzene (37).

We added 6.30 mL (15.9 mmol, 1.2 eq., 2.5M in Hexane) of *n*-BuLi dropwise to 3.20 g (13.2 mmol, 1.0 eq.) of the product (37) in dry THF at -78 °C under argon gas and stirred the mixture for 2 hours. 4.60 mL (4.15 g, 40.0 mmol, 3.0 eq.) of B(OMe)₃ was then added dropwise within 10 minutes at -78°C and the mixture stirred for 2 hours at -78°C, then overnight at room temperature. We extracted the solution with 100 mL of diluted 2N HCl and the product (38) recrystallized white under reduced pressure.

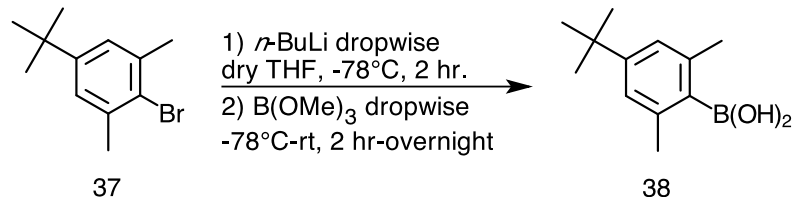


Figure 23. Addition of dihydroxy borate to compound 37 to produce product 38.

Up to this point, this synthesis was for the substituent group on the BINOL-base. The next step is connecting this substituent to the BINOL parent molecule.

To combine the parent BINOL with the substituent made above (product 38), we added 340 mg (0.600 mmol, 1.0 eq.) of (R)-3,3'-bisisod-2,2'-dimethoxy-1,1'-binaphthyl (BINOL) (39), 0.50 g (2.4 mmol, 4.0 eq.) of 4-*tert*-butyl-2,6-dimethylphenylboronic acid and 0.76 g (2.4 mmol, 4.0 eq.) of Ba(OH)₂·8H₂O together in a flask. We quickly added 70 mg (0.060 mmol, 10 mol%) Pd(PPh₃)₄ as the reaction catalyst. 24 mL of a solvent of DME (dimethyl ether)/H₂O (5/1) was added to these solids, then the mixture refluxed for 48 hours. We extracted the mixture with 1N HCl and CH₂Cl₂, concentrated the result under reduced pressure and purified the product (40 in Figure 24) through column chromatography (CH₂Cl₂/Hexane 1/7→1/1). The product 3,3'-(4-*tert*-butyl-2,6-dimethylphenyl)-2,2'-dimethoxy-1,1'-binaphthyl was confirmed by ¹H-NMR.

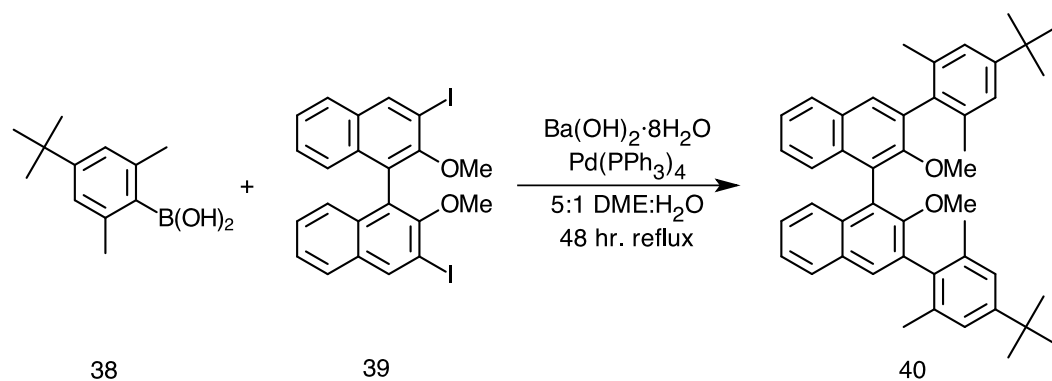


Figure 24. Combination of boronic acid derivative (38) to the BINOL base (39) to create the binaphthyl derivative (40).

The major structural components have been combined at this point and now the Brønsted acid part of the catalyst needs to be synthesized. To begin this process, we exchanged the methoxy groups (-OMe) for hydroxy groups (-OH): we slowly added a precooled solution of 0.75 mL (2.0 g, 7.9 mmol, 5.0 eq., dissolved in 8 mL abs. CH_2Cl_2) BBr_3 dropwise to a mixture of 1.00 g (1.58 mmol, 1.0 eq., dissolved in 60 mL abs. CH_2Cl_2) the product above (40) at 0°C under argon gas. The reaction stirred for 2 hours. Subsequently, we added 100 mL H_2O to the mixture at 0°C and let it stir for another 10 minutes before extracting the solution with CH_2Cl_2 and drying it over MgSO_4 . The product (41) was then concentrated under reduced pressure and purified over a silica column (CH_2Cl_2 :Hexane 1:4).

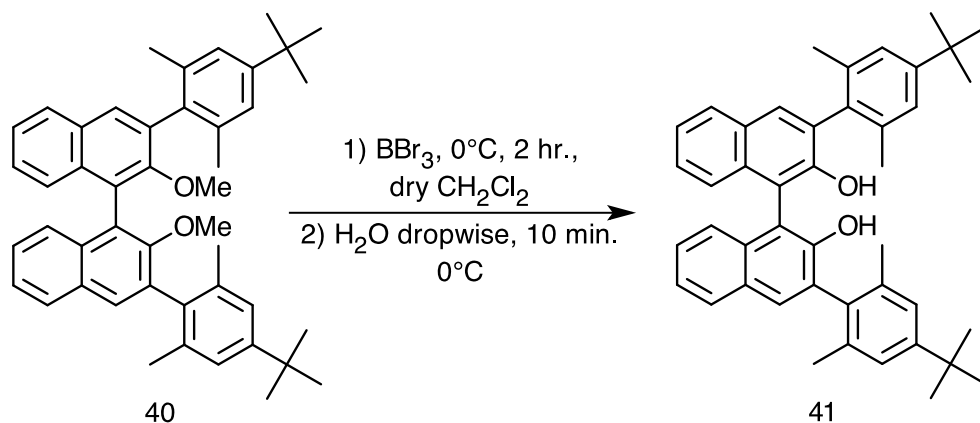


Figure 25. Substitution of methoxy groups (as in 40) for hydroxy groups (as in 41) on the BINOL-base.

The final step of this synthesis was to add the phosphoric acid to the BINOL base. We added 350 mg (0.570 mmol, 1.0 eq.) of our product (41) to 5 mL of absolute pyridine and cooled the mixture to 0°C under argon. We then added 160 μL (0.267 g, 1.74 mmol, 3.0 eq.) of POCl_3 to the flask and stirred the solution for 24 hours. Afterwards, we added 0.60 mL H_2O at 0°C and stirred another 24 hours. Subsequently we added 5 mL of 1N HCl to the reaction followed by a few mL of CH_2Cl_2 . We extracted the mixture with 1N HCl and CH_2Cl_2 and concentrated the solution under reduced pressure. The final catalyst (11) was a white powder that was stored at room temperature until needed.

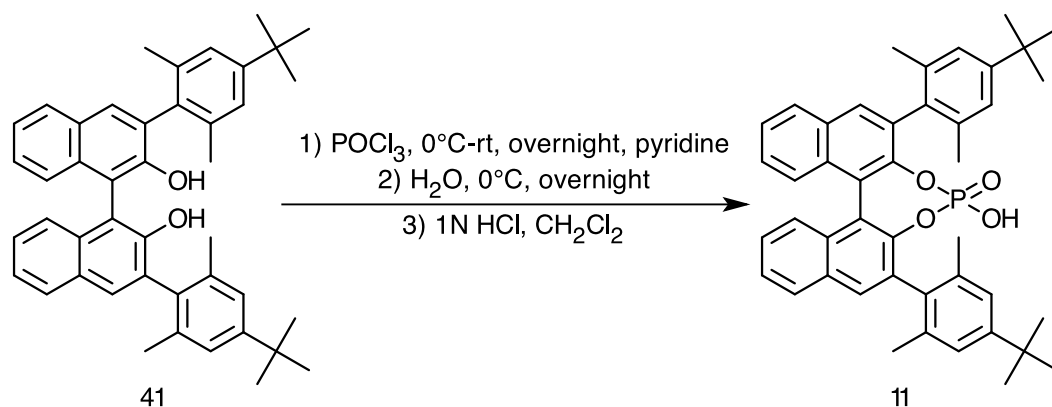


Figure 26. Addition of the phosphoric acid to the BINOL base (41) to form the final catalyst (11).

2.5 Final Three-Component Vinylogous Mannich Reaction

The synthesis of the chain product started with the formation of the imine. Under argon, we added 123 mg (1 eq., 1 mmol) of *p*-anisidine (9) to 3 mL dry THF and let the solution cool to -40 °C for 10 minutes. 128 mg (0.58 eq., 0.58 mmol) of the aldehyde (22) was then added in 3.25 mL of dry THF. We stirred the mixture and monitored the progress of the reaction through high pressure liquid chromatography (HPLC). After 2 hours of stirring, we added 67 mg (0.1 eq., 0.1 mmol) of the catalyst (11), let it stir for 10 minutes, then added 332 mg (1.405 eq., 1.405 mmol) of the dienolate nucleophile (10) dropwise to the reaction. We continued monitoring the reaction every 20 minutes by HPLC until the reaction appeared to reach completion, or the HPLC chromatographs did not change. After completion, the mixture turned cloudy with the addition of hexane. We concentrated the mixture under vacuum and prepared it for a silica gel

column. The purified product was identified as the predicted cyclic product (28) through the use of GC-MS, $^1\text{H-NMR}$, $^{13}\text{C-NMR}$, and HPLC (through comparison to a similar cyclical product). A different catalyst was also used for the 3-component reaction with all the same conditions as detailed above, but failed to yield our desired product.

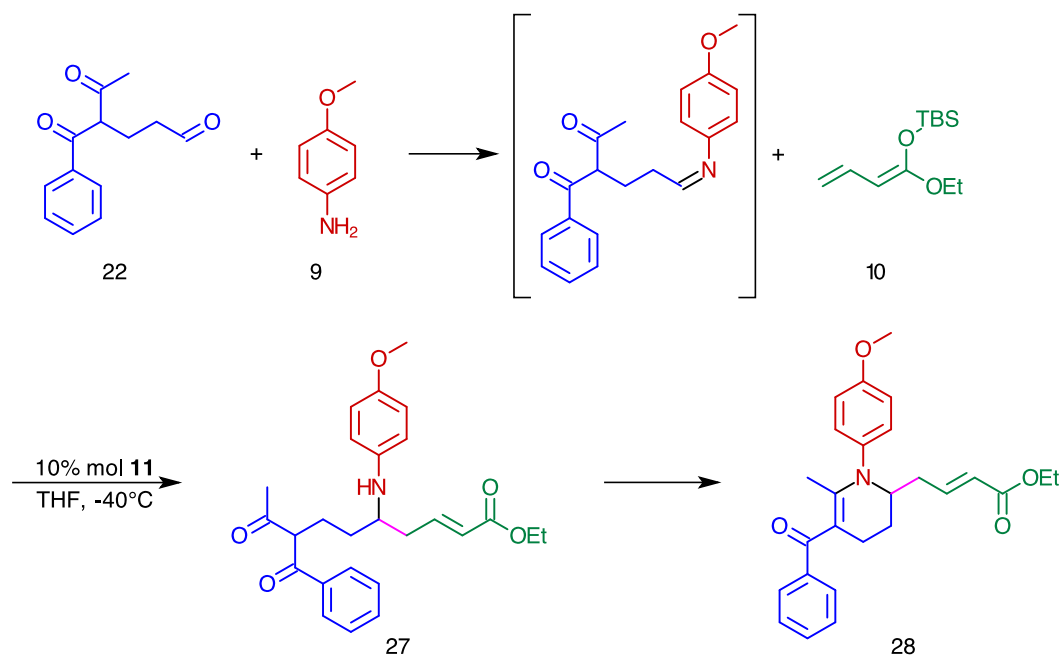


Figure 27. Thesis 3-component vinylogous Mannich reaction with aldehyde (22), amine (9), dienolate nucleophile (10) and the catalyst (11) to form the chain product (27), which then cyclizes to the final product (28).

2.6 Instrumentation and Materials

All solvents used were of technical grade. The NMR spectra were recorded on either a Varian Gemini 200 MHz (50 MHz), a Varian Mercury 300

MHz (75 MHz) or on a Bruker Avance DRX 400 MHz (100 MHz) instrument.

Infrared spectra were recorded on a Mattson/Unicam Genesis ATI spectrometer.

UV-VIS spectra were recorded on a Beckmann DU-650 spectrophotometer. Mass

spectra were recorded either on a Finnigan (EI) MAT 8230 or on a Bruker APEX

II FT-ICR (ESI). TLC plates from Merck (TLC silica gel 60 F254) were used.

Silica gel used for flash chromatography was Merck silica 60 (0.032 – 0.064 mm).

3. Results and Discussion

We synthesized the aldehyde, the dienolate, and the BINOL catalyst, three of the four molecules necessary for the vinylogous Mannich reaction. The fourth, the amine *para*-anisidine, was purchased and needed no further purification. In each of the syntheses, we confirmed the presence and purity spectroscopically and chromatographically. Because the dienolate and the catalyst were developed and frequently used in the Schneider lab group, the confirmation of the starting molecules was routine. The aldehyde and the final product of the vinylogous Mannich reaction however were unknown entities, and we obtained several different types of spectra to confirm the identities of each.

3.1 Identification of the Aldehyde 4-benzoyl-5-oxohexanal (22)

We attempted to synthesize our aldehyde with several different catalytic methods for the Michael reaction and a few different diketones including diethyl methyl malonate (42), diethyl malonate (43), ethyl acetoacetate (44), and benzoyl acetone (20). We used the Bartoli¹¹ method for each of these molecules first, which had limited success, then we tried a different method for synthesizing the 1,3 diketoaldehyde from Noël *et al.*²¹ using solid Al₂O₃ as a catalyst (Figure 28). Our use of the Noël method yielded little or no desired product. From both methods, most of the reactions yielded large amounts of side products and very

little, if any of the desired product. Only the benzoyl acetone with a $\text{CeCl}_3 \cdot 7\text{H}_2\text{O}/\text{NaI}$ (reaction (d) in Figure 28) produced a good yield (88%). After performing the Michael reaction with benzoyl acetone, we purified the aldehyde product (22) with silica gel column chromatography and identified the desired product using comparative TLC.

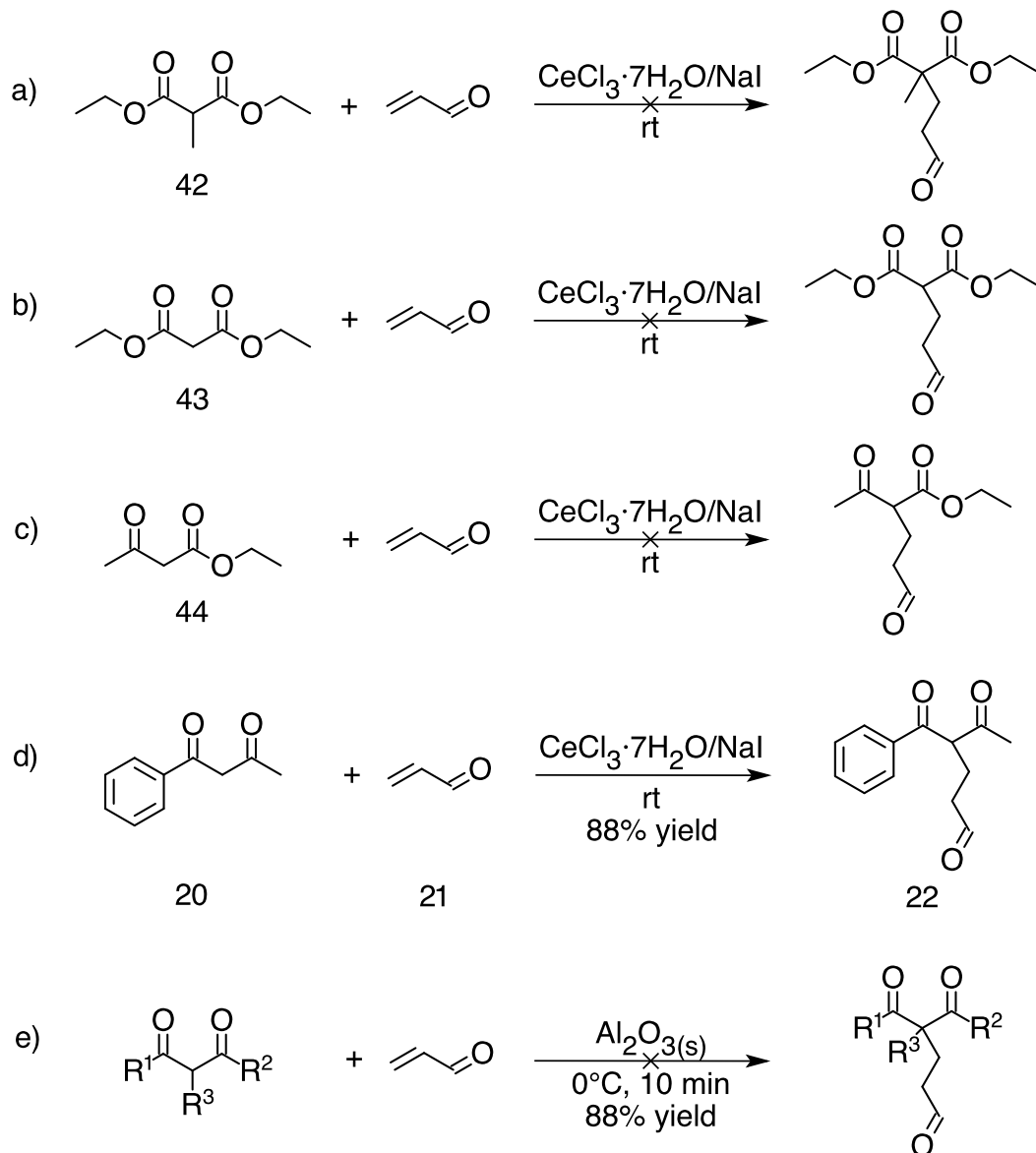


Figure 28. Aldehyde syntheses using various diketones and catalysts. Only the reaction with benzoyl acetone (d) produced a good yield (88%).

The IR spectrum confirmed the identity of the functional groups on the aldehyde (22) (Figure 29). Peak 1 in the functional group region, appears at a frequency for alcohols or amines though neither is present in our target molecule. The traditional alcohol vibrates around 3500 cm^{-1} and usually displays a strong broad peak on the spectrum. Similarly, amine bond between the nitrogen and hydrogen also vibrates with the same frequency but displays a medium but still broad peak. Peak 1 is a broad peak, but is relatively weak. Because our final aldehyde product contains a 1,3 diketone, we would expect the molecule to exhibit a tautomerized enol form. The weak peak probably corresponds to the alcohol on the tautomerized enol form on carbons 7 or 9. Peak 2 absorbs at the normal frequency for sp^2 carbons attached to hydrogens. Because our sample contains benzene (according to our predicted structure), the hydrogen bonds with the sp^2 carbons (2-6) of the benzene create this peak. Peak 3 similarly corresponds to sp^3 carbons attached to hydrogens, which we can see in our molecule as being on carbons 8, 10, 11, and 12. Because our final product contains an aldehyde, we expect to see two peaks at 2700 and 2800 cm^{-1} . Peaks 4 and 5 match our prediction of an aldehyde hydrogen (carbon 13). Between 1800 and 2000 cm^{-1} , we can observe some small peaks, which are characteristic frequencies of a benzene ring. The two strong peaks 6 and 7 correspond to carbonyl groups. One might believe that there are only two carbonyls from the two peaks, but the three carbonyl groups on our predicted product suggest that two of our three carbonyl peaks overlap. The two carbonyl peaks correspond to the carbonyls on carbons 7, 9, and 13. Peaks 8, 9, 10 and 11 match with carbon-carbon double bond

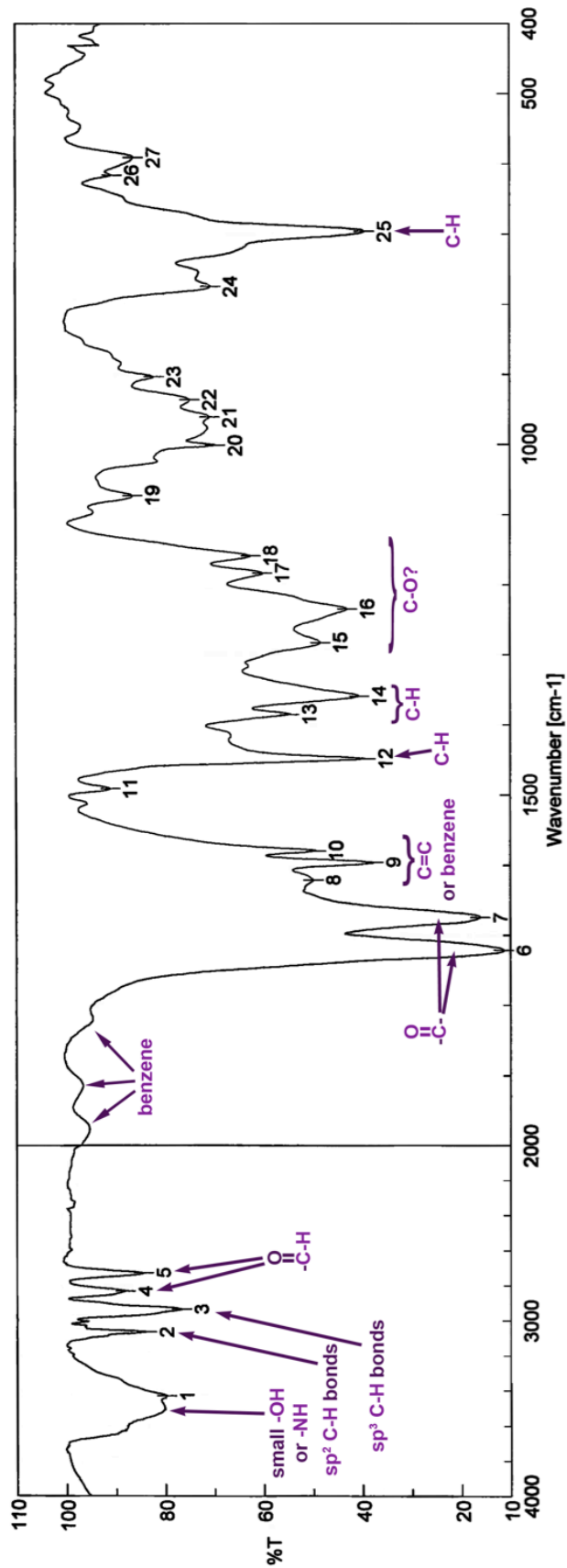


Figure 29. The IR spectrum for the aldehyde (22).

frequencies from the benzene and the enol rearrangement of the 1,3 dicarbonyl. Peak 12 corresponds to a carbon-hydrogen bending vibration, which would be found on carbons 8,10, 11, and 12.

The peaks between 1400 and 400 cm^{-1} mark the fingerprint region. The peaks in this region match typical absorptions for bending vibrations. Because of the wide variety of bending vibrations in larger molecules, the fingerprint region is usually harder to analyze. In this aldehyde spectrum, peaks 13 and 14 could be, similar to peak 12, from carbon-hydrogen bending vibrations of the methyl group on carbon 10. Peaks 15-18 might contain a carbon-oxygen stretching vibration from the enol rearrangement and peak 25 could also be a carbon-hydrogen bending vibration from the benzene.

From this analysis, we can determine that our molecule contains some sp^2 carbons, sp^3 carbons, and aldehyde, a benzene ring and at least 2 carbonyl groups. These all are consistent with our predicted aldehyde structure.

The $^1\text{H-NMR}$ spectrum is also consistent with the proposed structure of the aldehyde (Figure 30). From our predicted structure, we can already start formulating the spectrum of the $^1\text{H-NMR}$. For example, we would expect the hydrogens on the benzene ring (carbons 2-6) to show several multiplet peaks slightly above 7 ppm. We would also expect a relatively large triplet peak from the aldehyde hydrogen (carbon 13) shifted far downfield around 9 or 10 ppm. The methyl group, carbon 10, would most likely have a chemical shift around 2 ppm and be conspicuous as an integrated three-hydrogen singlet. From the 1,3 diketone structure and the subsequent acidity of the middle carbon, we can predict that the

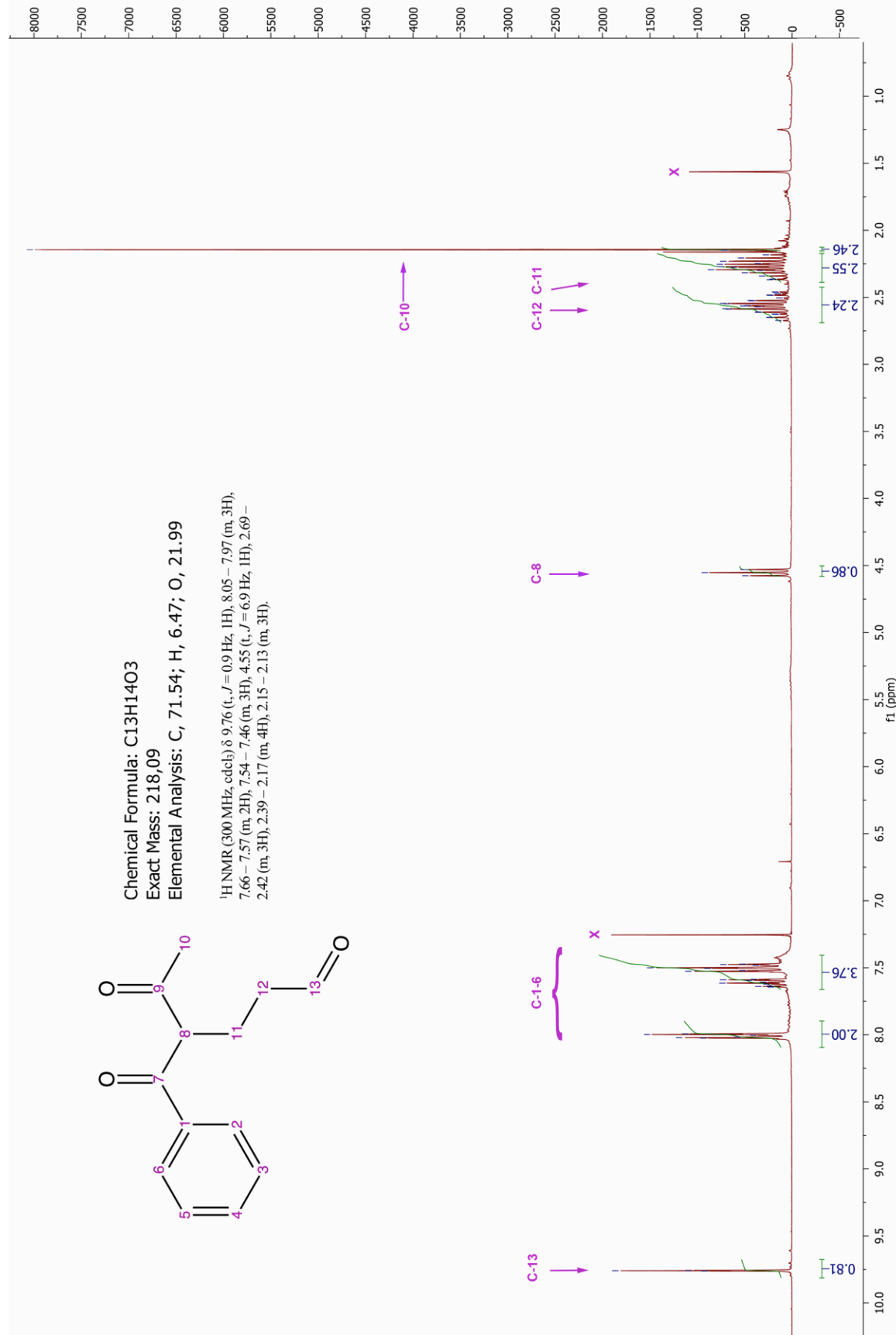


Figure 30. The ¹H-NMR spectrum for the aldehyde (22).

hydrogen on carbon 8 would have a chemical shift higher than 3 ppm and would show a triplet splitting pattern. We predict that the hydrogens on carbons 11 and 12 would show multiplet peaks around 2 ppm and possibly little difference between their respective shifts.

Looking at the $^1\text{H-NMR}$ spectrum the peak at 9.76 ppm corresponds to the aldehyde hydrogen on carbon 13 and is split into a triplet as expected. The typical vicinal coupling constant of around 1 Hz on this hydrogen is caused by the two adjacent hydrogens of carbon 12. We can also confirm that the peaks at 8.01, 7.61 and 7.50 ppm correspond to the five aromatic hydrogens from our predictions. At 4.55 ppm we can identify the single hydrogen residing on carbon 8. The vicinal coupling to the hydrogens on carbon 11 generates this peak as triplet with typical coupling constant of 7 Hz (Figure 31a). The hydrogens on carbons 12 and 11 correspond to the peaks found at 2.56 and 2.25 ppm respectively and are split into multiplets (as seen in Figure 31b). Because carbon 12 is found next to a carbonyl, this can explain how this carbon is more deshielded than carbon 11. Additionally, the high complexities of the signals are explainable with the diastereotopic character of each methylene group caused through the adjacent chiral center; whereby both protons of carbons 11 and 12 could appear as a doublet of double doublets. The carbon 10 hydrogens show a strong singlet around 2.14 ppm as we predicted. The two peaks labeled X are solvent peaks of CDCl_3 and hexane.

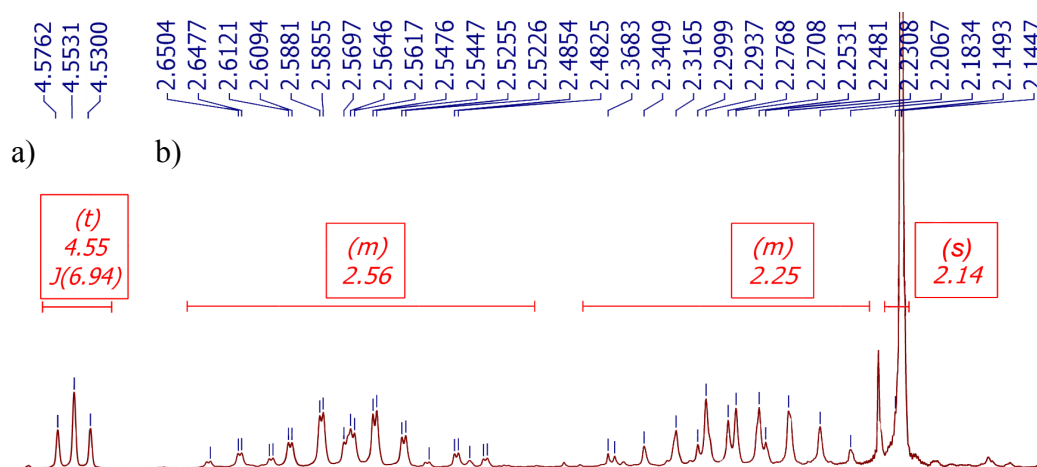


Figure 31. Peaks from the ¹H-NMR of the aldehyde. a) triplet peak at 4.55 ppm from the hydrogen on carbon 6; b) multiplet peak from the hydrogens on carbon 12 at 2.56 ppm, multiplet peak from the hydrogens on carbon 11 at 2.25 ppm and the singlet from the hydrogens on carbon 10 at 2.14 ppm.

The analysis of this spectrum is consistent with our predicted structure of the aldehyde, although it shows no sign of the tautomerized enol form of the 1,3 dicarbonyl group. The absence of peaks for this form is unsurprising. The tautomeric exchange is rapid on the NMR time scale at room temperature, and so the tautomer form is not observed.²²

Similar to the other spectra, the ¹³C-NMR spectrum also matches the predicted spectrum for our aldehyde (Figure 32). The carbon NMR has a similar pattern distribution of chemical shifts to the proton NMR. From our predicted structure, we can expect three peaks downfield that correspond to our three carbonyl groups in the aldehyde. The peak seen at 201.20 ppm is shifted far downfield, indicating it is a carbonyl carbon and likely carbon 13. The two peaks at 203.72 and 196.38 ppm are also in the carbonyl range and should match carbon

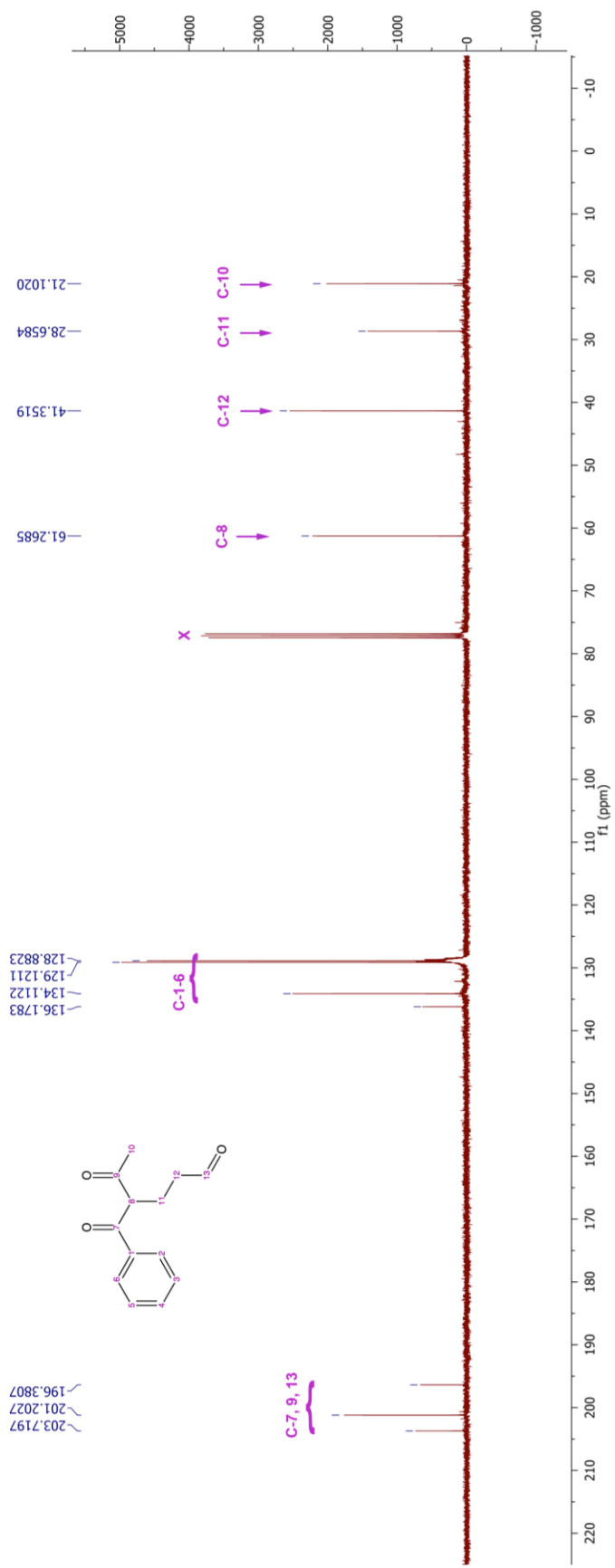


Figure 32. The ¹³C-NMR spectrum for the aldehyde (22).

12 and carbon 11 (not necessarily respectively). Four distinct benzene carbon resonances are observed between 125-140 ppm. Most likely, carbon 1 and 4 are found at 136.18 and 134.11 ppm, while carbons 2, 3, 5 and 6 are found at 129.12 and 128.88 ppm. Because carbon 8 is in an electron poor region due to the two carbonyl groups flanking it, we expect to see the peak to be seen between 50 and 80 ppm. Sure enough, a peak is seen at 61.27 ppm, which matches our prediction for the methyl carbon 8. We expect to find carbons 10, 11 and 12 between 10 and 50 ppm. These three peaks might be difficult to identify due to their similar carbon environments and the lack of splitting. The peak at 41.35 ppm is most likely carbon 12 because of the carbons position next to the aldehyde carbonyl in the molecule, which makes carbon 11 the peak at 28.66 ppm. The last peak at 21.10 ppm then by process of elimination must be carbon 10. The triple peak labeled X is the solvent peak of CDCl_3 . In this spectrum there is little evidence of the rearrangement of the 1,3 diketone, but the analysis agrees with our structure of the aldehyde.

We were additionally able to identify peaks in the mass spectrum that agreed with our predicted aldehyde structure (Figure 33). The molecular ion peak can be seen at 217.1 m/z and the base peak is seen at 105.1. The base peak corresponds to the mass of the phenyl group with the carbonyl $[\text{PhCO}]^+$. The prominent peak at 175 m/z corresponds to the 1,3 diketone groups with one of the alkane carbons from the aldehyde chain $[\text{PhCOCHCH}_2\text{COCH}_3]^+$ (Figure 33). The peaks at 77.1 and 51.1 m/z are characteristic of a benzene ring splitting.

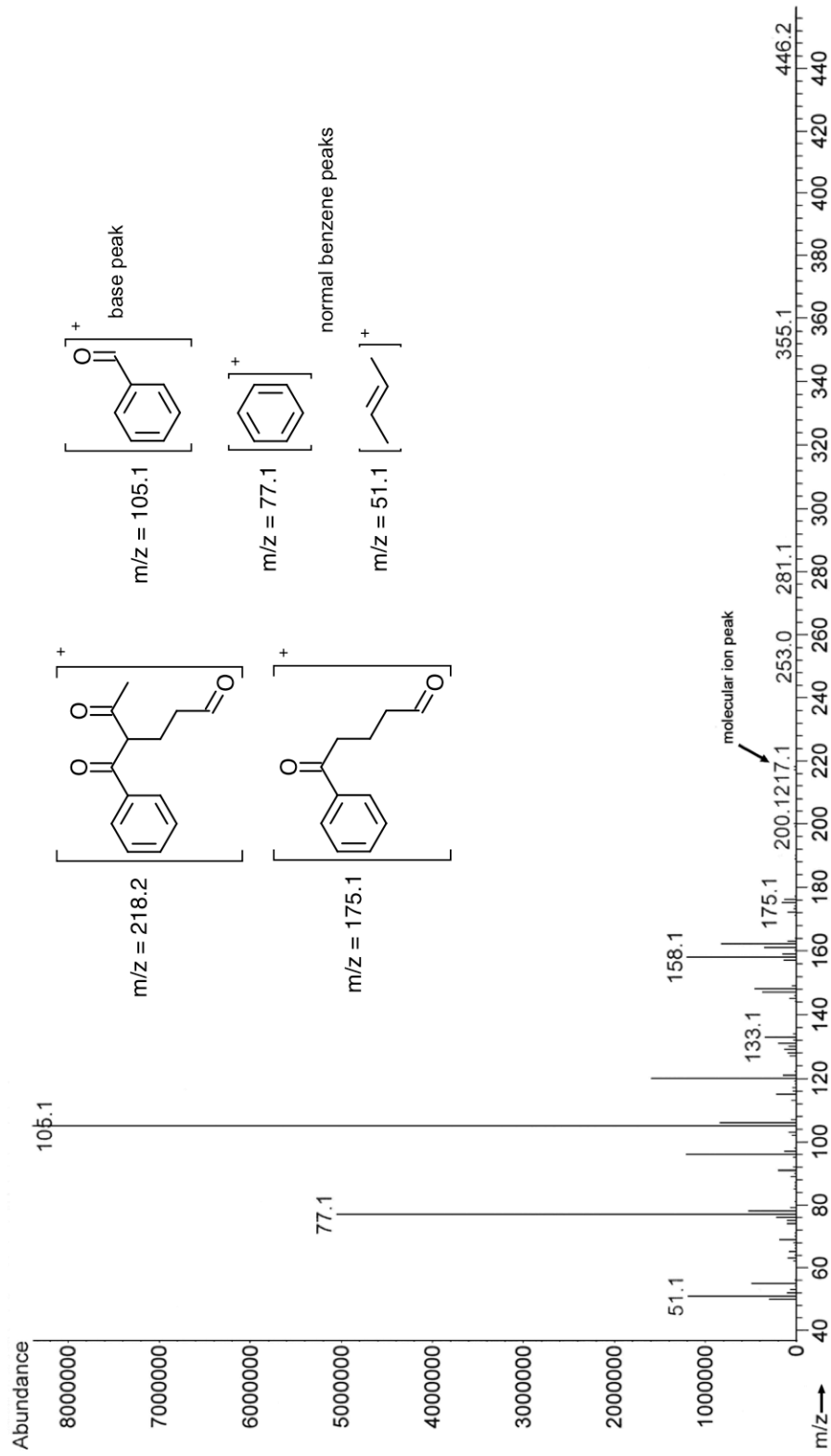


Figure 33. The ^{13}C -NMR spectrum for the aldehyde (22).

The mass spectrum for the aldehyde does contain some peaks that cannot be assigned, such as at 133.1 m/z and 158.1 m/z, but most of the peaks correlate to our predicted structure of the aldehyde and the predicted splitting.

3.2 Reaction Yields of the Dienolate Synthesis and the Catalyst Synthesis

The lab group of Professor Schneider developed the synthesis for the dienolate nucleophile and reported the yields (as seen below) for each step of the reaction.

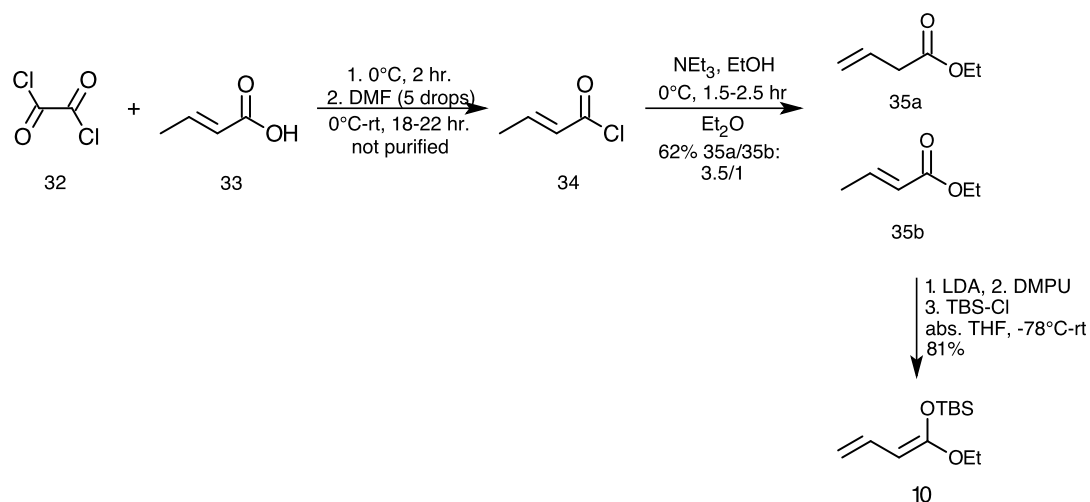


Figure 34. The synthesis of the dienolate nucleophile with yields.

The Schneider lab group determined that the first step of the reaction between the oxalyl chloride (32) and crotonic acid (33) to form crotonyl chloride (34) required no purification before continuing the synthesis. The reaction of crotonyl chloride produced a yield of 62% of the two desired products (35) with a ratio of 3.5/1 between 35a/35b. These two products, after the previous reaction,

reacted with LDA, DMPU, and TBS-Cl resulted in an 81% yield of the final dienolate nucleophile product (10).

The catalyst synthesis, like the dienolate synthesis, was developed by the Schneider group and the reported yields from each step of the synthesis were as follows:

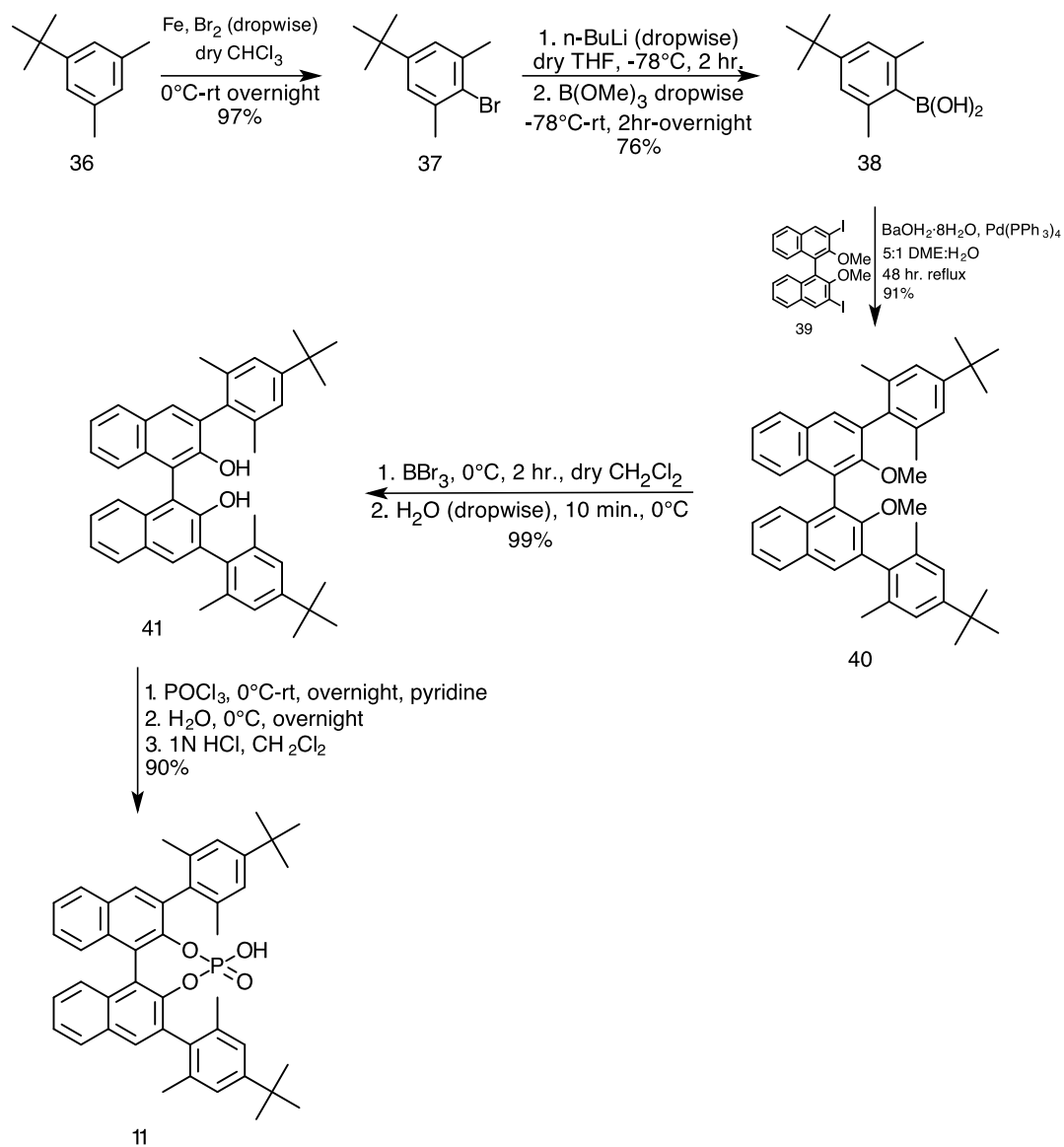


Figure 35. The BINOL catalyst synthesis with yields.

The first reaction we performed in the synthesis of the catalyst was the addition of bromine to the substituted benzene (36). This reaction gave us a high yield of 97%. We further combined this product with trimethoxy boron to get a yield of 76% of the boronic acid derivative (38). This derivative reacted with the BINOL base (39) to produce 91% yield of the binaphthyl derivative (40). We produced a high yield of 99% from the further synthesis to the hydroxy substituted BINOL base. The last reaction, the addition of the phosphoric acid, yielded 90% of the desired product.

3.3 Monitoring of the Imine Formation via HPLC Analysis in the Final Vinylogous Mannich Reaction

When performing the final vinylogous Mannich reaction with the four components (aldehyde, amine, dienolate, and catalyst), we monitored the reaction progress chromatographically. We started by monitoring the imine formation from the reaction between the aldehyde and the amine. After the two compounds were mixed in a test tube, a small sample of the mixture was diluted in hexane and analyzed by normal phase high-pressure liquid chromatography. We expected that the absorbance peaks for *para*-anisidine and the aldehyde in the HPLC would decrease in intensity as the two components were consumed and an imine peak would appear as the reaction progressed. We observed that this was in fact the case (Figure 36), but the peak thought to be the imine did not alter greatly between 20 minutes and 2 hours. From this we can say that the imine formed

quickly and that we could continue to the next step after a small amount of stirring.

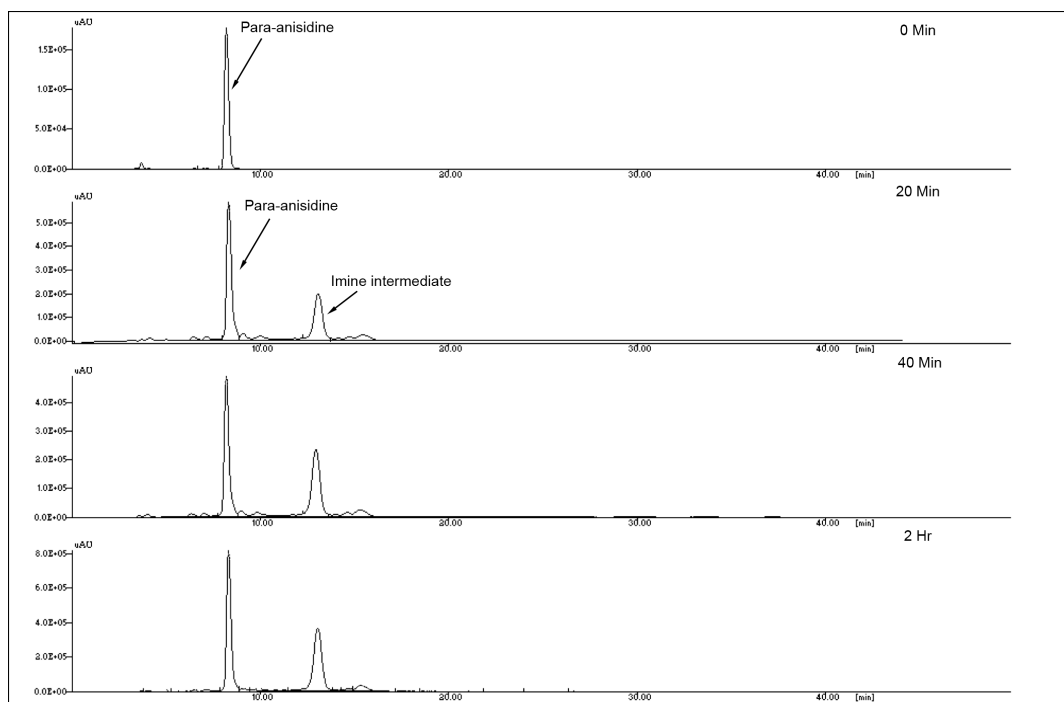


Figure 36. Chromatogram comparison at 220 nm. Top to bottom: 1) *para*-anisidine, 2) *para*-anisidine and aldehyde, 20 min. -40 °C, 3) *para*-anisidine and aldehyde, 40 min. -40 °C, 4) *para*-anisidine and aldehyde, 2 hr. -40 °C. The imine peak formed is seen at 13.052 min. Note that the aldehyde does not absorb at 220 nm. Note that the y-axes are differently scaled.

These chromatograms show primarily the formation of the imine. The *para*-anisidine (8.187 min) is the clear peak in the first chromatogram and it can be clearly seen in the following chromatograms as well. In the second chromatogram, after 20 minutes of stirring, the imine formation took place, and the imine product is the clear peak at 13.052 minutes with absorption maxima at 201, 243, and 285 nm. Interestingly, between 20 minutes of stirring and 2 hours of stirring, the ratios between the *p*-anisidine and formed imine do not change

significantly, so the imine forms quickly. Several side products were formed, which are visible at 8.402 min and 9.237 min with similar heights and absorption maxima of 203, 245, and 279 nm. Due to the excess amount of the amine component used it is not surprising to observe the signal of *p*-anisidine until the end.

After the imine formed, the catalyst and nucleophile were added to the reaction mixture. Like the imine monitoring, we monitored the reaction progress and the formation of our final product.

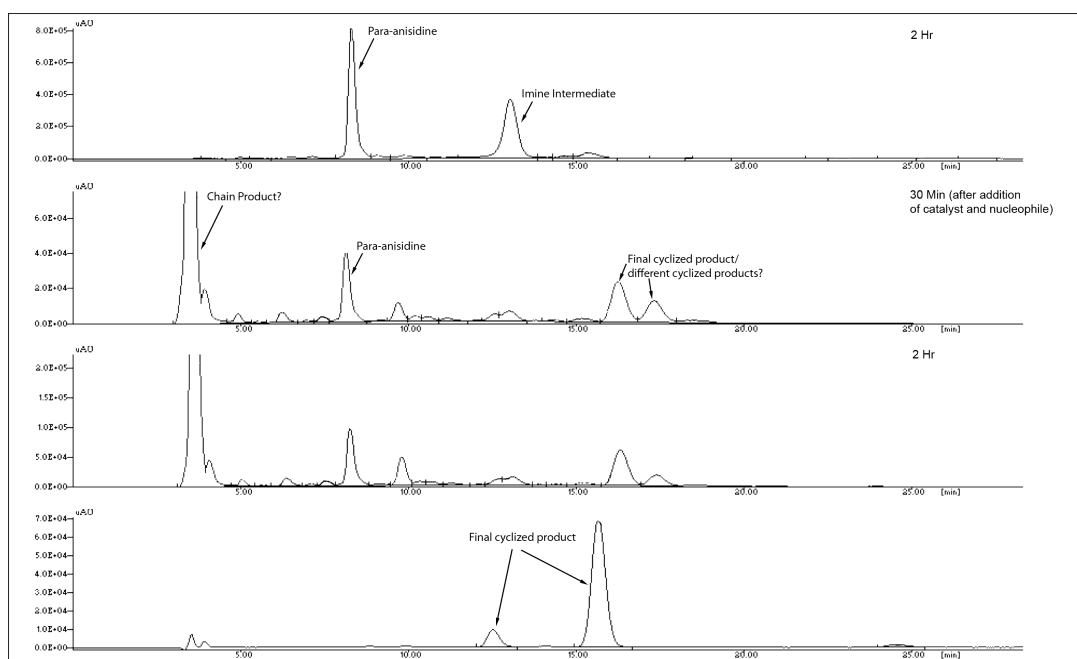


Figure 37. Chromatogram comparison at 220 nm. Top to bottom: 1) *para*-anisidine and aldehyde with imine product, 2 hr. -40 °C, 2) *para*-anisidine, aldehyde, phosphoric acid catalyst and dienolate nucleophile, 30 min. -40 °C 3) *para*-anisidine, aldehyde, phosphoric acid catalyst and dienolate nucleophile, 2 hr. -40 °C, 4) Final cyclized product. Note that the y-axes are differently scaled.

The chromatograms above allow us to compare the actual final product HPLC to the reaction of all four components. The final cyclized product can be identified in the last chromatogram as the two peaks at 12.52 minutes and 15.615 minutes. The second peak has UV maxima at 203, 243 and 337 nm. In the second and third chromatograms, we can observe the presence of the nucleophile at 4.32 minutes. This peak, at a high concentration in the mixture, has UV maxima at 197, 221, 237, 307, and 323 nm. We can also identify the *para*-anisidine through all the reaction chromatograms as the major peak at 8.234 minutes. The smaller signals in the second and third chromatograms could originate from the open chain form of the vinylogous Mannich product, a similar cyclized product, or side products. The peak at 15.964 minutes in the second and third chromatograms has the same UV traces as our final cyclized product and the shift of this peak could be explained by a variation in solvent polarity from the reaction mixture. Intriguingly, the peak at 17.039 minutes also has similar UV maxima. This UV trace similarity could indicate a different extinction coefficient of our desired product in the column, or could be identifiable as a different cyclized product.

3.4 Identification of the Cyclized Product

When beginning the final vinylogous Mannich reaction, instead of using the BINOL-based phosphoric acid, we started by using a similar catalyst, diphenylphosphate (Figure 38). This phosphoric acid has the same catalytic center

as the BINOL-based acid used in the final reaction, but has free phenyl groups instead of the locked BINOL-base.

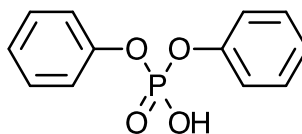


Figure 38. Diphenylphosphate was the first catalyst used in our complete vinylogous Mannich reaction.

The use of diphenylphosphate yielded messy HPLCs with many side products. We also observed none of our desired and predicted product (28). After reverting to the BINOL-based catalyst, we observed the presence of our predicted product with 83% *ee*. This final product produced a heterocyclic ring, allowing us to generically name the product tetrahydropyridine.

In addition to monitoring the vinylogous Mannich reaction with HPLC, we confirmed the presence of our predicted final cyclized product using various spectroscopic and spectrometric techniques. The $^1\text{H-NMR}$ of the cyclized product (Figure 39) confirms the identity of our final product and also the manner in which the chain product cyclized.

Starting downfield, the clusters of peaks around 7.5 ppm and 6.9 ppm distinctly indicate two benzenes. We can distinguish between the two benzenes based on the splitting patterns. The mirror image pattern on the peaks at 6.9 indicates a para-substituted benzene, which is what we expected in the para-methoxyphenyl group on the nitrogen. The hydrogens from these benzene peaks

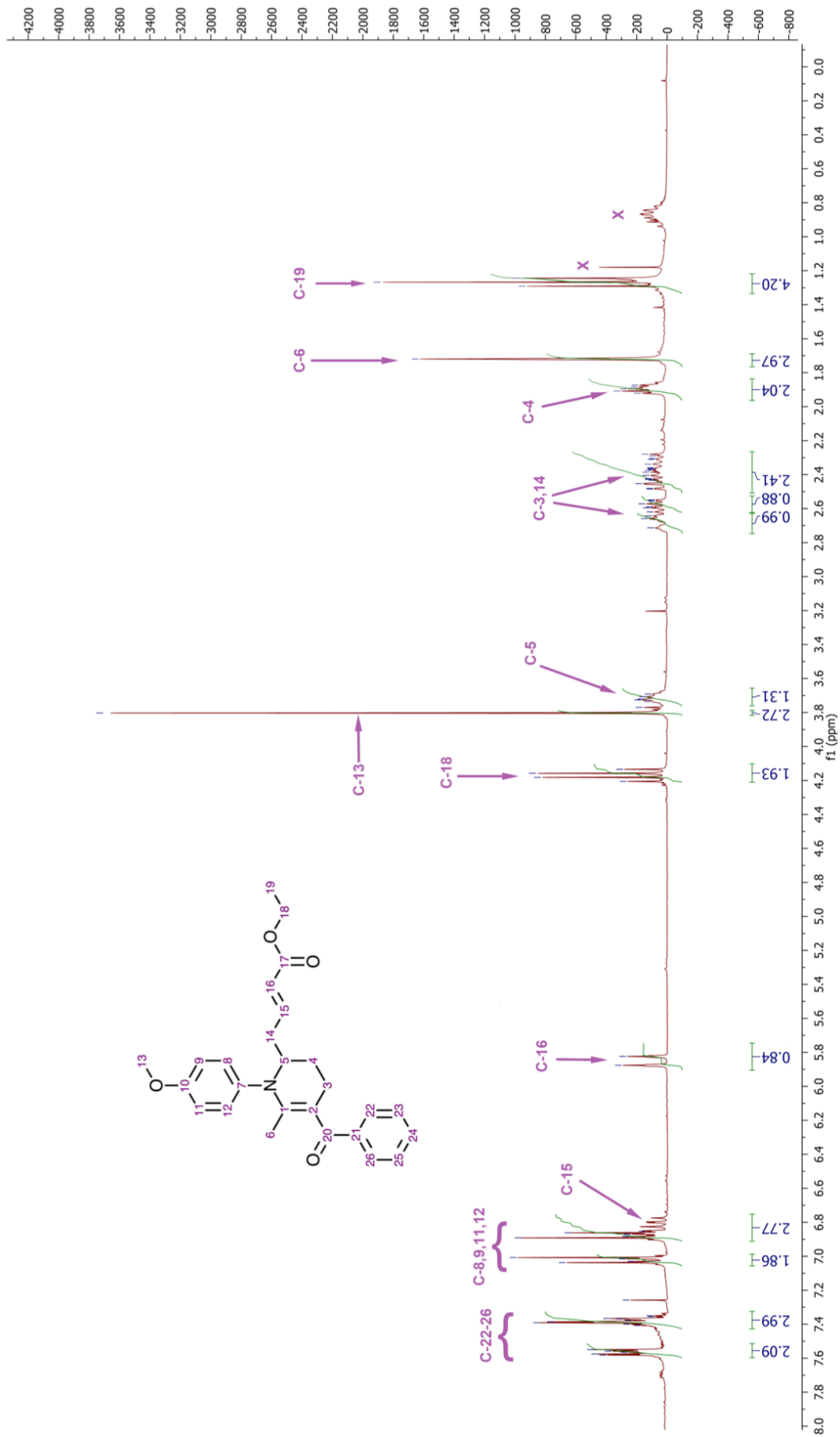


Figure 39. The ¹H-NMR spectrum for the cyclized product (28).

are the ones present on carbons 9, 10, 12 and 13. Logically, this means that the other benzene hydrogens clustered around 7.5 are the hydrogens on the benzoyl group, on carbons 22-26. We specifically looked for a pair of peaks corresponding to the hydrogens on carbons 15 and 16. We predicted that carbon 16 would be split into a doublet and have a fairly high shift between 5 and 6 due to the presence of the ester next to it and the resonance between the olefin and the carbonyl. Similarly we expected to see carbon 15 as a multiplet in the same range as the benzene hydrogens. One might be surprised to observe that carbon 15 absorbs a higher frequency than carbon 16, since carbon 16 is closer to the carbonyl. However, since the carbonyl contributes to the resonance hybrid of the olefin, carbon 15 carries a partial positive charge, making it less shielded than its neighbor and therefore it absorbs at a higher frequency. The multiplet at 6.8 ppm that overlaps with some benzene peaks speaks to being carbon 15 as we predicted and the doublet at 5.8 ppm, corresponding to carbon 16, similarly confirms our proposed structure. Continuing upfield, we can identify the quartet at 4.1 ppm to be carbon 18, split by the hydrogens on carbon 19. The spectrum also includes a triplet peak further downfield in the methyl region that corresponds to carbon 19. The singlet at 3.8 ppm could at first glance correspond to a couple of different carbons in our molecule: carbon 6 and carbon 13, since both are expected to give singlets. After determining that the shift of carbon 6 would probably be closer to 2 since it is not next to an electrophilic atom, we can determine that this large singlet peak matches carbon 13. The multiplet at 3.7 ppm indicates another alkane carbon next to an electrophilic atom. In this case, the position of the nitrogen and

the relatively low integration indicates that this peak is from the hydrogens on carbon 5.

From this point, the peaks are all alkanes. We predict to see carbon 6 as a singlet around 2 ppm, and carbon 19 as a triplet. Because carbons 3 and 14 have similar environments, we are unable to distinguish the two, but we can rationalize they will both be more deshielded than carbon 4 since they are next to olefinic carbons. Keeping this in mind, we can determine that all the multiplet peaks around 2.5 are carbons 3 and 14. Similarly, the multiplet peak at 1.9 ppm can be matched with carbon 4. As predicted, the peak at 1.7 ppm corresponds to carbon 6, and the triplet seen at 1.3 ppm matches the carbon 19 hydrogens (*vide supra*). Solvent impurity peaks in our ^1H NMR are labeled with X.

The ^1H -NMR spectrum for the final molecule is particularly important, because it can distinguish between two different cyclized products that were possible from our reaction. We predicted that a majority of the product would cyclize as we have been discussing, but another cyclization pathway was equally possible, where the benzoyl group and carbon 7 are reversed (Figure 40). The position of the singlet of carbon 7 in our ^1H -NMR shows that our predicted cyclized product is in fact the one we isolated. If the other product was formed, the hydrogen shift of carbon 7 would be closer to 2.4 ppm, rather than at 1.7 ppm, which is the location of the peak in our spectrum.

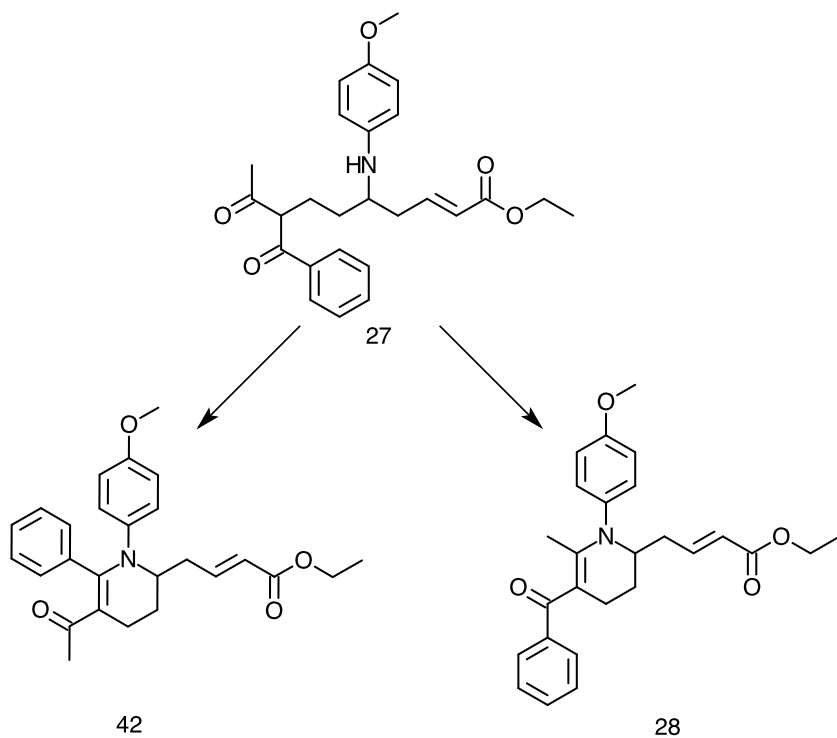


Figure 40. The two most likely cyclizations from the chain product.

The ^{13}C NMR spectrum (Figure 41) is more difficult to interpret than the proton NMR. One useful clue to identifying the respective peaks is seen in the positioning of the peaks in the spectrum. This specific carbon NMR spectrum is an APT spectrum. When looking at the spectrum, the peaks above the 0 baseline (positive peaks) carry an even number of hydrogens (0 or 2) and the peaks below the 0 baseline (negative peaks) carry an even number of hydrogens (1 and 3). By looking at the compound, the first prediction we can make is the presence of two peaks at a high field between 180 and 200 ppm. These two peaks would correspond to the two carbonyl groups on carbons 20 and 17 and would show positive peaks on the spectrum, since they have an odd number of hydrogens (0). We expect the carbon 20 carbonyl to be shifted farther downfield due to the

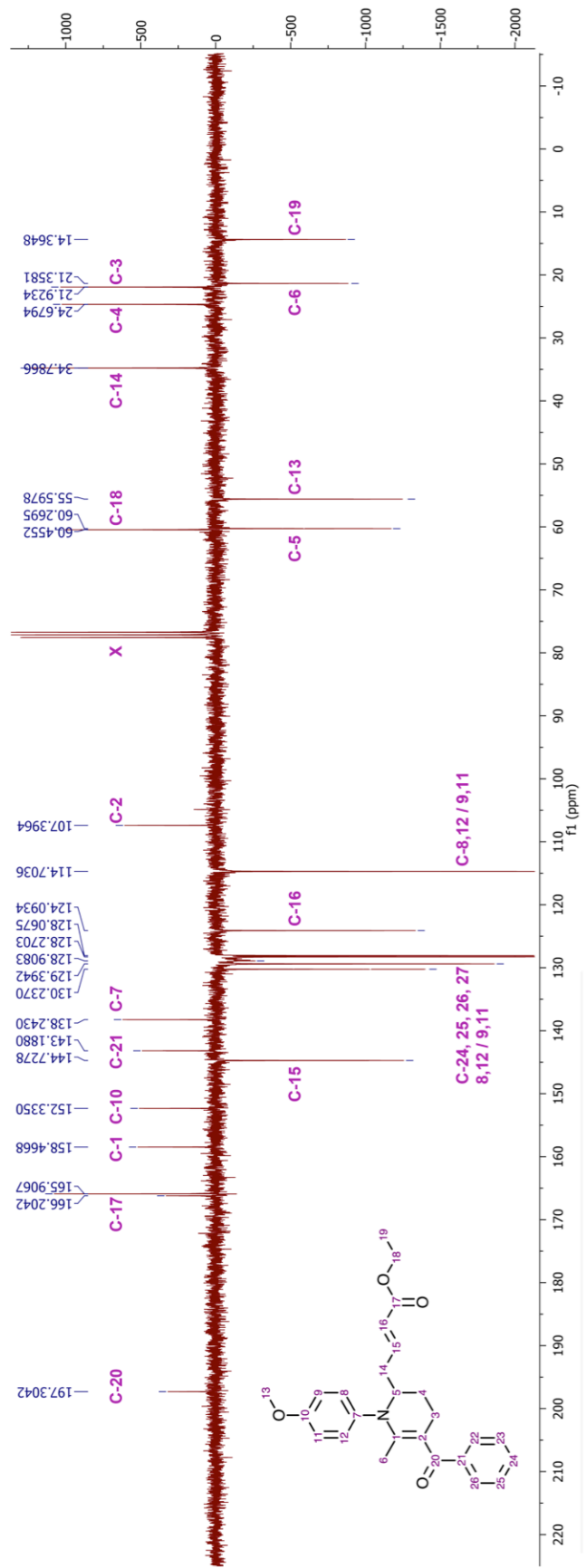
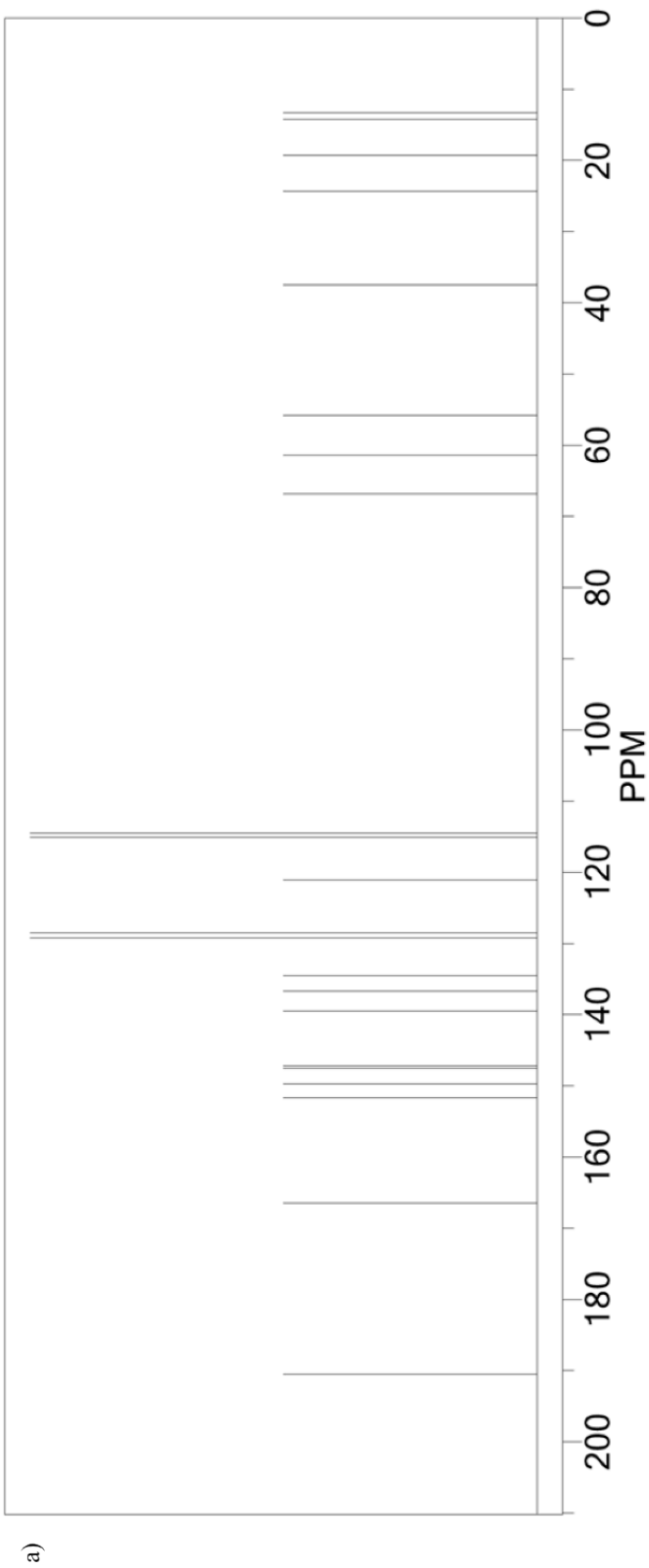


Figure 41. The ¹³C-NMR spectrum for the cyclized product (28).

highly conjugated system surrounding it. Indeed two high peaks that are most likely these two carbons occur at 197.3 ppm and at 166.2 ppm. The cluster of peaks below the baseline around 130 ppm is reminiscent of benzene carbons. All of these peaks are likely to be the hydrogen-carrying carbons on both of the benzene rings in our molecule. We expect that carbons 1, 2, 7, 10, and 21 to be shifted downfield and to display positive peaks, since each of these have no hydrogens and are part of a conjugated system. Similarly, carbons 15 and 16 should be found downfield, but display negative peaks, which is indicative of the single hydrogen on each of these carbons. Carbons 3, 4, 14 and 18 are not part of a conjugated system and therefore are expected to be more shielded and further upfield. All these carbons should also exhibit positive peaks, since each of these carbons holds two hydrogens. Likewise, we expect carbons 5, 6, 13, and 19, which all carry an odd number of hydrogens and are not part of a conjugated system, to show negative peaks between 0 and 70 ppm.

Due to the large number of carbons in our compound and the absence of splitting in the carbon NMR spectrum, we can use chemical drawing software to generate a prediction of the ^{13}C -NMR spectrum (Figure 42). Some of the peaks between the generated spectrum and the actual spectrum (Figure 41) differ greatly; however, the generated spectrum gives us a rough estimate of the expected chemical shift of each. With the assistance of this model, we were able to differentiate some peaks.



b) ChemNMR ^{13}C Estimation

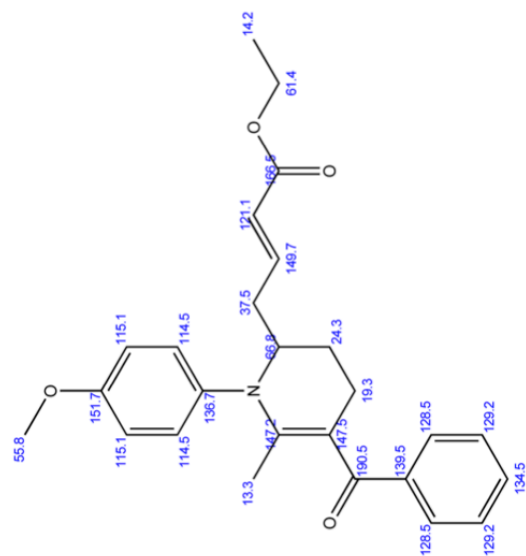


Figure 42. a) The ^{13}C -NMR prediction spectrum for the cyclized product (28). b) The predicted shifts for the cyclized product.

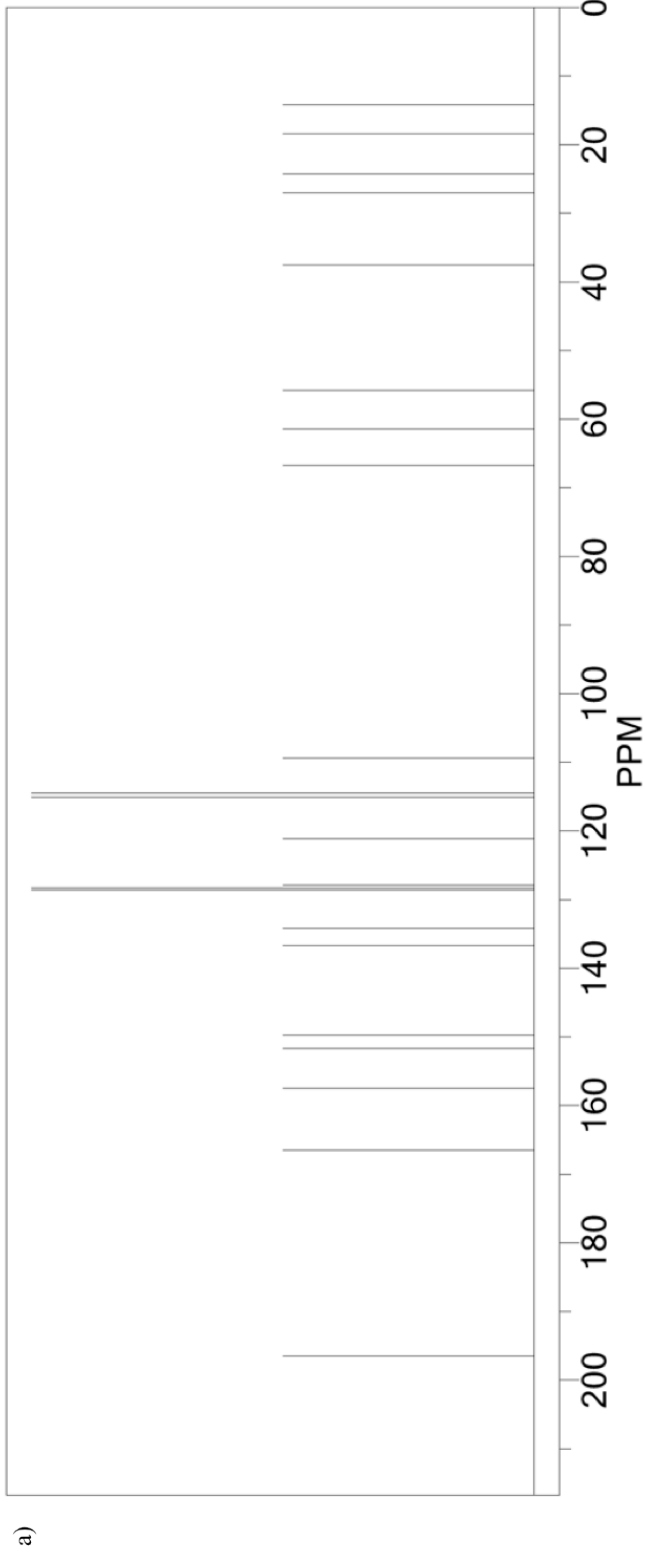
Estimation quality is indicated by color: good, medium, rough

Our generated ^{13}C -NMR spectrum predicts that carbon 20 and carbon 17 will shift chemically at 190.5 ppm and 166.5 ppm respectively. We expect these high shifts due to the electron-withdrawing properties of the oxygen in both of the carbonyls. We can identify the two carbonyl peaks at 197.3 and 166.2 ppm in our product spectrum. The next four positive carbon peaks in our predicted spectrum do not readily match up with peaks seen in our actual spectrum, but can be used as general guidelines for identifying each peak. Our predicted spectrum indicates that carbon 10 has a high shift of 151.7 ppm followed by the twin peaks of carbons 1 and 2 at 147.2 and 147.5 ppm respectively, and also carbon 21, which has a predicted shift of 139.5 ppm. These predictions do not readily correspond to the peaks in our actual spectrum, making it very difficult to say for certain which peaks are which. Carbon 1 is in the middle of a conjugated system and is directly next to an electron withdrawing nitrogen, which makes us believe that this carbon can be identified as absorbing at 158.3 ppm. The peak found at 152.3 ppm is likely carbon 10, since it is a benzene carbon and also is neighbored by an electronegative oxygen. Carbon 21, being part of a benzene ring and next to a conjugated carbonyl, is likely to be the peak at 143.2 ppm. Though the generated spectrum predicts carbon 2 to have a relatively high chemical shift, we believe that this carbon actually corresponds to the peak at 107.4 ppm. The peak at 138.24 ppm on our spectrum nicely corresponds to the predicted shift of carbon 7. This relatively high chemical shift is due to the neighboring electronegative nitrogen atom as well as the deshielding effects of the benzene ring.

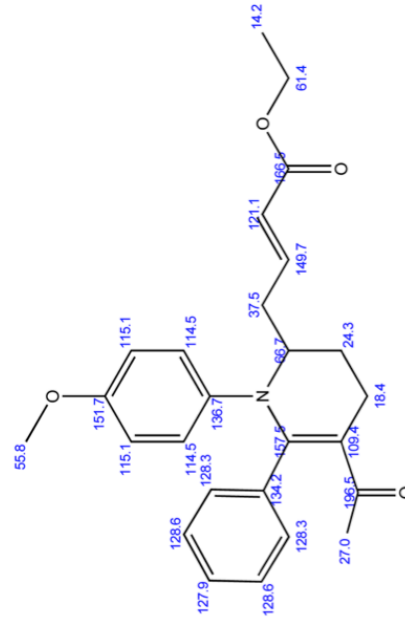
Looking at the negative downfield peaks in our product spectrum, we can identify the peak at 144.7 ppm as carbon 15. This carbon is relatively deshielded due to the slightly positive charge it carries from the resonance with the carbonyl. The other carbon of the double bond, carbon 16, can be seen farther upfield at 124.09 ppm. The other peaks in the area, including the peaks between 131 and 127 ppm, are where we expect to see all of our various benzene peaks. We can safely say that this cluster includes carbons 22-26 and possibly also carbons 8 and 12 or 9 and 11. The peak at 114.7 ppm presents a slight puzzle, considering it is not grouped with the benzene peaks and is less shielded than the double bonded carbon 16; however, this peak probably corresponds to two of the four carbons on the PMP benzene near the nitrogen. Because this benzene has 2 hydrogen environments, we can assume that this large peak is due to either carbons 8 and 12 or to carbons 9 and 11. Below the three CDCl₃ solvent peaks labeled X, we can see a group of three peaks around 60 ppm. All three of the carbons in question (carbons 18, 5 and 13) are shifted downfield from the neighboring oxygens or nitrogen atoms. Our generated spectrum predicts these peaks to be carbon 5 at 66.8 ppm, carbon 18 at 61.4 ppm and carbon 13 at 55.8 ppm. These numbers correspond fairly well with our analysis, and we determined that carbon 18 has a chemical shift of 60.46 ppm, that carbon 5 has a shift at 60.27 ppm and that the peak at 55.6 matches with carbon 13. We can distinguish between carbon 18 and carbon 5 based on the number of hydrogens on each carbon. Carbon 18 has two hydrogens and therefore displays a positive peak, whereas carbon 5 has three hydrogens, making it a negative peak. Carbon 14 is a normal methyl carbon with

two hydrogens next to a double bond and in the middle of the molecule. From this information, we can deduce that it will display a chemical shift between 30 and 40 ppm and will show a positive peak. The peak at 34.79 matches this deduction and can therefore be labeled as carbon 14. Carbons 3 and 4 have very similar environments and cannot easily be distinguished. Based on guidance from the predicted spectrum and the reasoning that carbon 3 is next to a double bond, we judged that the peak at 24.68 ppm matches carbon 3 and that carbon 4 corresponds to the next peak at 21.92 ppm. The last two carbons, carbons 6 and 19, were also fairly difficult to differentiate since both have similar environments. Based upon a similar argument to that presented above, we deduced that the peak at 21.36 ppm corresponds to carbon 6, since it is influenced by the flow of electrons through the nearby conjugated system, leaving carbon 19 to be the very shielded peak at 14.36 ppm.

The use of NMR prediction software can be useful in confirming and identifying peaks in spectra, but the generated spectra cannot be entirely relied upon, since they are mathematical calculations and cannot take all the environmental considerations into account. For example, our actual carbon spectrum can also be made to match the constitutional isomer discussed above (Figure 40), and the generated spectrum for the isomer is more consistent with our actual spectrum (Figures 41 and 43). Further data is required to absolutely confirm the structure of our product. For this confirmation we turned to NOESY NMR, which allowed us to look more specifically at which carbons were close in proximity to one another (Figure 44).



b) ChemNMR ¹³C Estimation



Estimation quality is indicated by color: good, medium, rough

Figure 43. a) The ¹³C-NMR prediction spectrum for the second possible cyclized product (28). b) The predicted shifts for the second possible cyclized product.

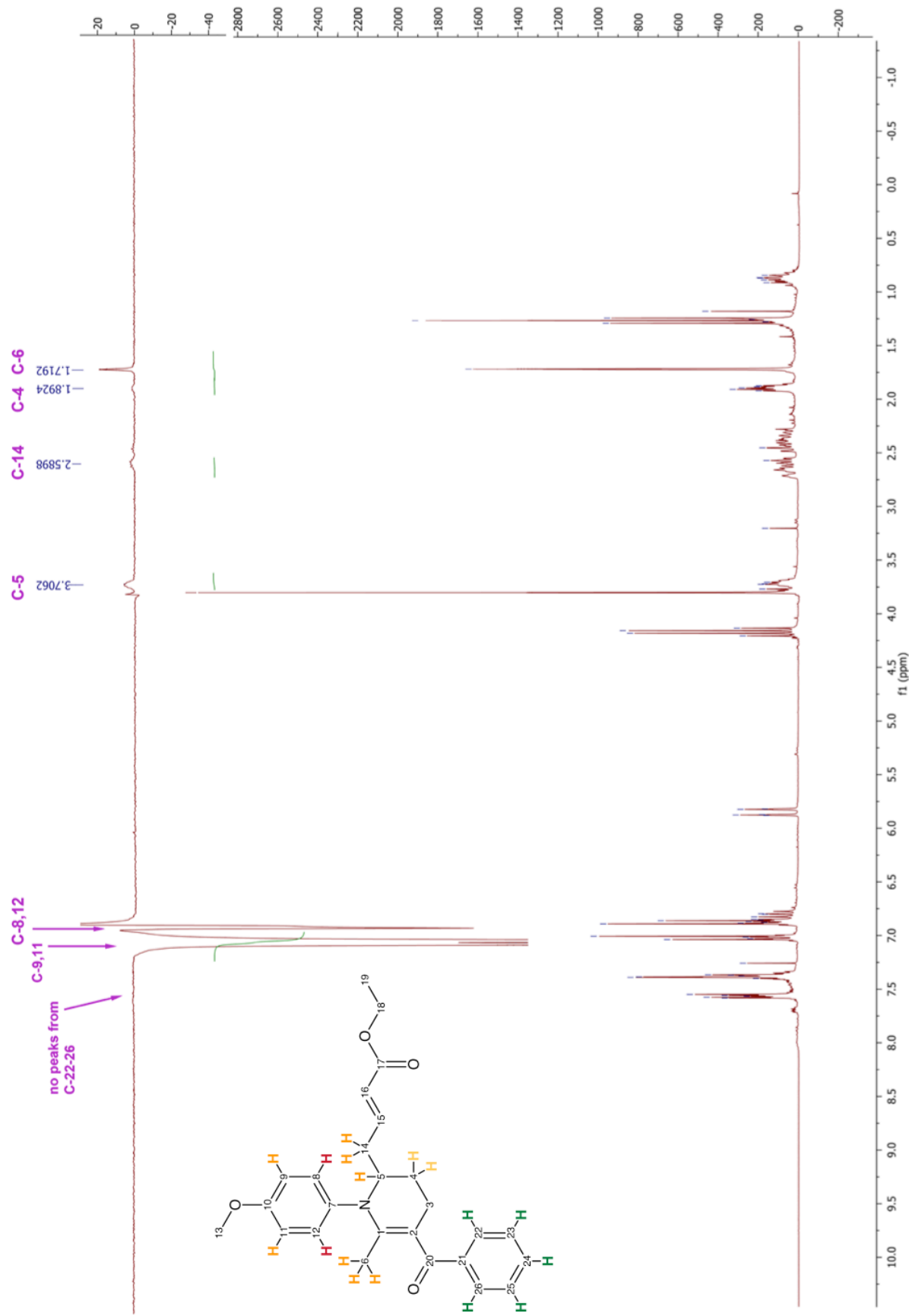


Figure 44. The NOESY spectrum above the ¹H-NMR spectrum for the cyclized product (28) exciting hydrogens on carbons 8 and 12. The red labeled hydrogens on the molecule are excited and excite the orange labeled (and the yellow to a lesser extent) hydrogens. The green labeled hydrogens (and those hydrogens not shown) are not in close enough proximity to be excited.

In our NOESY spectrum, we specifically excited the two hydrogens on carbons 8 and 12. As these excited hydrogens relaxed to their original spin state, they excited several hydrogens in the vicinity. These hydrogens similarly relaxed back to their original spin state and emitted frequencies that were detected by the NMR. From speculation, we asserted that the two hydrogens on carbons 8 and 12 (in red in Figure 44) would excite the hydrogens on carbons 5, 6, 9, 11, and 14 (in orange), since they are the closest in proximity to carbons 8 and 12. Our spectrum shows four peaks that do indeed correspond to our predicted structure and assertion. We observe a peak at 3.71 ppm, which matches carbon 5, as we discussed in the ^1H NMR spectrum. The second peak is at the chemical shift where we deduced the hydrogens of carbons 3 or 14 would show. Because the carbon 14 hydrogens are some of the hydrogens predicted to couple with our NOESY excited hydrogens, we can deduce that the set of peaks shifted farther downfield are in fact from the carbon 14 hydrogens. There is a small peak at 1.89 ppm, which is the chemical shift we determined was for the carbon 4 hydrogens. This suggests that the NOESY excited hydrogens on the benzene couple slightly with the carbon 4 hydrogens. The largest peak of the four peaks is at 1.72 ppm. As stated above, this singlet peak corresponds to the hydrogen attached to carbon 6. This peak above all others confirms our belief that our predicted structure is correct. Were our product actually the isomer instead (Figure 40), the NOESY peak at 1.72 ppm would not appear, since the NOESY excited hydrogens would not be in the proximity of the methyl group. In its place the hydrogens on the additional benzene ring (in green) would display peaks, which they do not. This

NMR method allowed us to definitively determine that our cyclic product of the vinylogous Mannich reaction matched our predictions of a heterocyclic product.

Our mass spectrum of the final product also matches with our predicted structure (Figure 45). The molecular ion peak can be seen at 419.3 m/z and our base peak can be identified at 306.2 m/z. This base peak is consistent with the loss of the methyl ether chain from the heterocycle. Other major peaks include the loss of ethyl from the ether substituent, resulting in a peak at 390 m/z, the loss of the ethoxy group of the ether substituent, which displays a peak at 374.2 m/z, and the peak at 346.3 m/z, which corresponds to a loss of the ether completely (Figure 45). The peaks at 200.1 m/z and 122.1 m/z result in a loss of both the ether substituent chain and the PMP group on the nitrogen, with an additional loss of the second phenyl for the latter peak. The three peaks at 105.0, 77.0 and 51.0 m/z are characteristic of benzene ring splitting.

The spectra for our final product confirm that our predicted product for the vinylogous Mannich reaction formed. Additionally, we measured 83% enantioselectivity in our product. Unfortunately, no yield was determined for this experiment, as we were primarily concerned with verifying the presence of the product.

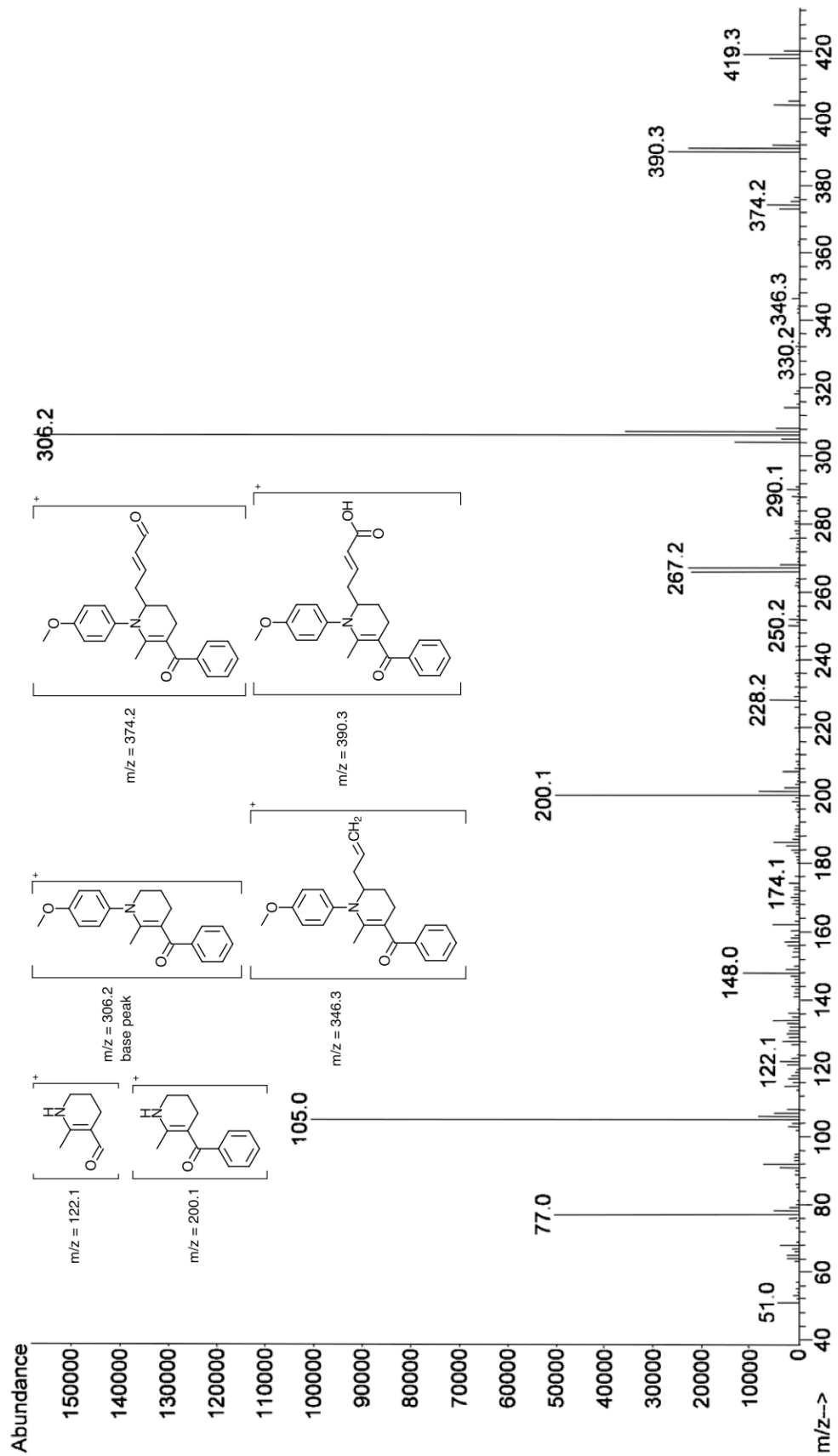


Figure 45. The mass spectrum for the final product (28)

4. Conclusions

Organic chemists strive to create molecules at high levels of yield and enantioselectivity in the laboratory. Using building blocks of atoms, chemists find new combinations and reactions for these elements. One of the most difficult and desirable foci in organic chemistry is the creation of a carbon-carbon bond in a molecule. Several different reactions have been developed throughout history, which yield high amount of product and stereospecificity, but we are always looking for easier, cheaper, and more efficient ways to carry out these reactions. The vinylogous Mannich reaction provides high yield, high enantioselectivity products for the difficult problem of forming a carbon-carbon bond.

In this thesis, we investigated varying the aldehyde in a 3-component vinylogous Mannich reaction with a BINOL-based phosphoric acid catalyst. The investigation of differing 1,3-diketoaldehydes for the 3-component vinylogous Mannich reaction led to the synthesis of 4-benzoyl-5-oxohexanal (22) through the use of the Michael reaction. This reaction produced relatively high yields (88%) and a stable product that could be easily stored for later use. The BINOL-based catalyst used in this reaction was optimized in the Schneider lab group and stereospecifically catalyzed the vinylogous Mannich reaction into the final product, a tetrahydropyridine derivative. The heterocyclic product of this reaction is a useful product and can possibly be used as an intermediate in a natural or synthetic product synthesis. The most important information this reaction presents

is how to make such a compound and a possible solution to creating similar products.

Further work on this reaction would include optimizing the yield of the reaction, since it generated a fairly low yield, and also improving the enantioselectivity above the current 83% *ee*. This reaction enhancement can be accomplished by varying the reagent amounts, changing the reaction temperature and timing, or even changing the catalyst to another similar BINOL-based molecule.

The general vinylogous Mannich reaction can also be further studied and the mechanism for the catalytic cycle investigated. Varying the reagents, such as the aldehyde and the amine in this reaction, allows us to learn more about the limitations and peculiarities of this reaction. Additionally, we can investigate the mechanism of this reaction so as to better understand the chemistry behind it and be able to direct the reaction more successfully toward our desired products. The investigation of chemicals and organic synthesis is evident in everyday life in such areas as pharmacy, biodegradables, and materials. The more we can learn about the reactions to create these products and the mechanisms behind them, the more medicines and innovative products we can create and develop for our best interests.

5. References

- (1) Grabley, S., and Thiericke, R. (1999) *Drug Discovery from Nature*. Berlin: Springer.
- (2) Landoni, M.F., and Soraci, A. (2001) Pharmacology of Chiral Compounds 2-Arylpropionic Acid Derivatives. *Curr. Drug Meta.* **2**, 37-51.
- (3) Corey, E. J. (2002) Catalytic Enantioselective Diels-Alder Reactions: Methods, Mechanistic Fundamentals, Pathways, and Applications. *Angew. Chem., Int. Ed.* **41**, 1650-667.
- (4) Bruice, P. Y. (2001) *Organic Chemistry*. Upper Saddle River, NJ: Prentice Hall.
- (5) Smith, M. B., and March, J. (2007) *March's Advanced Organic Chemistry: Reactions, Mechanisms, and Structure*. **6th ed.** Hoboken, NJ: Wiley-Interscience.
- (6) Davis, F. A., Chao, B. and Rao, A. (2001) Intramolecular Mannich Reaction in the Asymmetric Synthesis of Polysubstituted Piperidines: Concise Synthesis of the Dendrobate Alkaloid (+)-241D and Its C-4 Epimer. *Org. Lett.* **3**, 3169-171.
- (7) Sickert, M., Abels, F., Lang, M., Sieler, J., Birkemeyer, C. and Schneider, C. (2010) The Brønsted Acid Catalyzed, Enantioselective Vinylogous Mannich Reaction. *Chem.—Eur. J.* **16** 2806-818.
- (8) Kryshstal, G. V., Kulganek, V. V., Kucherov, V. F. and Yanovskaya, L. A. (1979) Phase-Transfer Catalysis of the Michael Addition to α,β -Unsaturated Aldehydes. *Synthesis* **1979** 107-09.
- (9) Bartoli, G., Bartolacci, M., Bosco, M., Foglia, G., Giuliani, A., Marcantoni, E., Sambri, L. and Torregiani, E. (2003) The Michael Addition of Indoles to α,β -

Unsaturated Ketones Catalyzed by $\text{CeCl}_3 \cdot 7\text{H}_2\text{O}$ –NaI Combination Supported on Silica Gel. *J. Org. Chem.* **68**, 4594-597.

- (10) Bartoli, G., Bosco, M., Bellucci, M., Marcantoni, E., Sambri, L. and Torregiani, E. (2001) Conjugate Addition of Amines to α,β -Enones Promoted by $\text{CeCl}_3 \cdot 7\text{H}_2\text{O}$ –NaI System Supported in Silica Gel. *J. Org. Chem.* **66**, 9052-055.
- (11) Bartoli, G., Bosco, M., Bellucci, M., Marcantoni, E., Sambri, L. and Torregiani, E. (1999) Cerium(III) Chloride Catalyzed Michael Reaction of 1,3-Dicarbonyl Compounds and Enones in the Presence of Sodium Iodide Under Solvent-Free Conditions. *Eur. J. Org. Chem.* **1999**, 617-20.
- (12) Martin, S. F. (2002) Evolution of the Vinylogous Mannich Reaction as a Key Construction for Alkaloid Synthesis. *Acc. Chem. Res.* **35**, 895-904.
- (13) Liu, T., Cui, H., Long, J., Li, B., Wu, Y., Ding, L. and Chen, Y. (2007) Organocatalytic and Highly Stereoselective Direct Vinylogous Mannich Reaction. *J. Am. Chem. Soc.* **129**, 1878-879.
- (14) Casiraghi, G., Battistini, L., Curti, C., Rassu, G. and Zanardi, F. (2011) The Vinylogous Aldol and Related Addition Reactions: Ten Years of Progress. *Chem. Rev.* **111**, 3076-154.
- (15) Zhang, Q., Hui, Y., Zhou, X., Lin, L., Liu, X. and Xiaoming Feng. (2010) Highly Efficient Asymmetric Three-Component Vinylogous Mannich Reaction Catalyzed by a Chiral Scandium(III)- N,N' -Dioxide Complex. *Adv. Synth. Catal.* **352**, 976-80.
- (16) Denmark, S. E. and Beutner, G. L. (2003) Lewis Base Activation of Lewis Acids. Vinylogous Aldol Reactions. *J. Am. Chem. Soc.* **125**, 7800-801.
- (17) Sickert, M. and Schneider, C. (2008) The Enantioselective, Brønsted Acid Catalyzed, Vinylogous Mannich Reaction. *Angew. Chem., Int. Ed.* **47**, 3631-634.

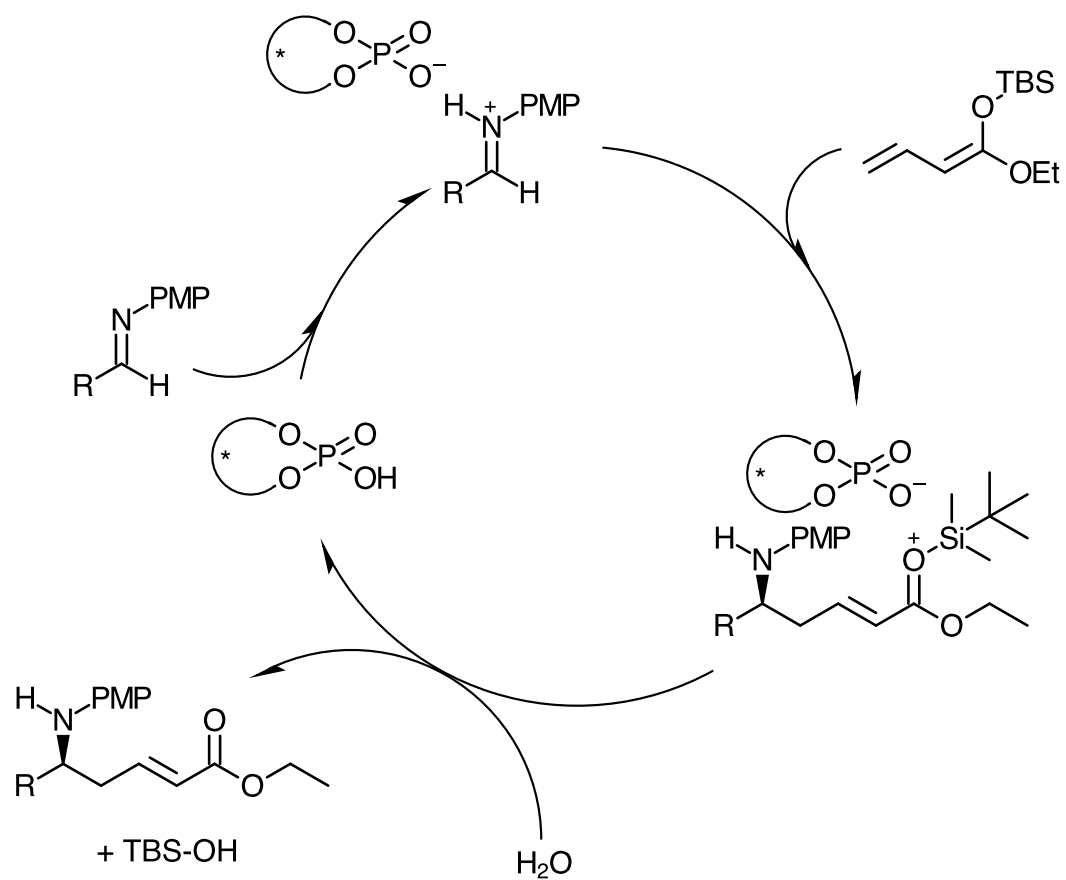
- (18) Uraguchi, D. and Terada, M. (2004) Chiral Brønsted Acid-Catalyzed Direct Mannich Reactions via Electrophilic Activation. *J. Am. Chem. Soc.* **126**, 5356-357.
- (19) Akiyama, T., Morita, H. and Fuchibe, K. (2006) Chiral Brønsted Acid-Catalyzed Inverse Electron-Demand Aza Diels–Alder Reaction. *J. Am. Chem. Soc.* **128**, 13070-3071.
- (20) Akiyama, T., Itoh, J. and Fuchibe, K. (2006) Recent Progress in Chiral Brønsted Acid Catalysis. *Adv. Synth. Catal.* **348**, 999-1010.
- (21) Akiyama, T., Itoh, J., Yokota, K. and Fuchibe, K. (2004) Enantioselective Mannich-Type Reaction Catalyzed by a Chiral Brønsted Acid. *Angew. Chem., Int. Ed.* **43**, 1566-568.
- (22) Noël, R., Vanucci-Bacqué, C., Fargeau-Bellassoued, M. and Lhommet, G. (2005) Synthesis of New Chiral 6-Carbonyl 2,3,8,8a-Tetrahydro-7H-oxazolo[3,2-a]pyridines. *J. Org. Chem.* **70**, 9044-047.
- (23) Crossley, M. J., Field, L. D., Harding, M. M. and Sternhell, S. (1987) Kinetics of Tautomerism in 2-substituted 5,10,15,20-tetraphenylporphyrins: Directionality of Proton Transfer between the Inner Nitrogens. *J. Am. Chem. Soc.* **109**, 2335-341.
- (24) Arend, M., Westermann, B. and Risch, N. (1998) Modern Variants of the Mannich Reaction. *Angew. Chem., Int. Ed.* **37**, 1044-070.
- (25) Ranu, B. C. and Bhar, S. (1992) Surface-mediated Solid Phase Reaction: Dramatic Improvement of Michael Reaction on the Surface of Alumina. *Tetrahedron* **48**, 1327-332.
- (26) Wieland, L. C., Vieira, E. M., Snapper, M. L. and Hoveyda, A. H. (2009) Ag-Catalyzed Diastereo- and Enantioselective Vinylogous Mannich Reactions of α -

Ketoimine Esters. Development of a Method and Investigation of Its Mechanism. *J. Am. Chem. Soc.* **131**, 570-76.

6. Supplemental Material

Table I. Position and intensity of peaks in IR spectrum for the aldehyde (22)

Number	Position (cm ⁻¹)	Intensity (%T)
1	3427.85	79.6742
2	3063.37	83.7501
3	2933.2	76.6717
4	2829.06	88.0708
5	2726.85	84.4569
6	1721.15	11.3142
7	1674.87	16.1061
8	1620.88	49.8047
9	1595.81	37.6212
10	1579.41	49.2342
11	1490.7	90.8575
12	1448.28	39.1799
13	1384.64	54.6261
14	1358.6	40.4768
15	1282.42	48.2431
16	1234.22	42.8588
17	1183.11	60.0063
18	1159.01	62.3923
19	1073.19	86.255
20	1000.87	69.5057
21	960.377	70.6931
22	936.271	74.676
23	903.487	81.9886
24	774.279	70.4608
25	696.177	39.622
26	616.145	90.4692
27	591.075	86.1241



The proposed catalytic cycle for the vinylogous Mannich reaction.⁷